Frontal structure and transport in the northwestern Weddell Sea

Andrew F. Thompson & Karen J. Heywood
School of Environmental Sciences, University of East Anglia, Norwich, U.K.

Submitted to Deep-Sea Research on September 24, 2007

corresponding author address:
Andrew F. Thompson
School of Environmental Sciences
University of East Anglia
Norwich, NR4 7TJ
United Kingdom
andrew.f.thompson@uea.ac.uk
ph: +44 1603 591424
fax: +44 1603 591327

Abstract

Hydrographic data from the Antarctic Drifter Experiment: Links to Isobaths and Ecosystems (ADELIE) project are analyzed to determine the frontal structure and transport along a section across the continental shelf and slope in the northwestern Weddell Sea. The flow is dominated by three barotropic northward flowing currents: the Antarctic Coastal Current, the Antarctic Slope Front and the Weddell Front. The strongest baroclinic flows are confined to the region between the Slope Front and the Weddell Front over the steepest part of the continental slope. The Antarctic Coastal Current flows over the continental shelf near a local steepening in the bathymetry and has a transport of $\sim$1.3 Sv. The Antarctic Slope Front is found approximately 25 km offshore of the shelf break in 800 m of water. The Slope Front, which is associated with a transport of $\sim$4 Sv, exhibits peak velocities at the sea bed that reach 35 cm s^{-1} as detected by lowered acoustic Doppler profiler (LADCP) measurements. A third, previously unreported northward current is found centered between the 2500 m and 3000 m isobath corresponding to a local break in the topography. There is evidence that this is the same feature known as the Weddell Front traditionally associated with flow over the 3000 m isobath in the northern Weddell Sea. The absence of the Weddell Front in data from pervious field programs is explained by too coarse or too shallow sampling. The Weddell Front accounts for $\sim$17 Sv of northward transport. A deep outflow is observed all along the continental slope between the Slope Front and the Weddell Front. The deep outflow is localized in two to three distinct cores that are tied to topographical features. The total transport across the section is 46 ± 6 Sv. This value exceeds previous estimates because the full-depth and de-tided LADCP measurements allowed the narrow ($\sim$20 km) frontal currents to be resolved, leading to more accurate estimates of the barotropic component of the flow. We discuss the physical processes that may lead to the formation and maintenance of these fronts.

1 Introduction

The flow behavior in the western Weddell Sea allows this region to play a disproportionately large role in the global thermohaline circulation. Ventilation of the deep ocean depends crucially on the production of dense water around Antarctica (Deacon 1937, Stommel and Arons 1960, Mantyla and Reid 1983, Orsi *et al.* 2002), especially in the western Weddell Sea, which accounts for 50-90% of Antarctic bottom water (Carmack 1977, Foldvik and Gammelsrød 1988, Rintoul 1998). The formation of bottom water can either occur through the interaction of High Salinity Shelf Water, resulting from brine rejection during sea ice formation, with Warm Deep Water and Winter Water (Foster and Carmack 1976, Middleton *et al.* 1987, Foster *et al.* 1987), or through the interaction of Ice Shelf Water, caused by glacial melt under ice shelves, with Warm Deep Water (Weiss *et al.* 1979, Foldvik *et al.* 1985*a*). In both cases, dense water originating on the continental shelf spills over the shelf break and proceeds to sink down the continental slope. The path of this dense water is subsequently influenced by topographical features, turbulent entrainment and the Coriolis effect (Baines and Condie 1998), which act together to form a series of fronts along the rim of the Weddell Gyre.

In near-surface waters, shelf-slope exchanges in the western Weddell Sea help control krill dynamics over large parts of the Southern Ocean. The western Weddell Sea is a region of enhanced chlorophyll relative to adjacent high nutrient, low chlorophyll waters found throughout most of the Southern Ocean (Falkowski *et al.* 1998). The high chlorophyll region extends from the tip of the Antarctic Peninsula northeastward to the South Sandwich Islands incorporating the Weddell-Scotia Confluence (Thorpe *et al.* 2004). Elevated chlorophyll levels result from high nutrient content on the continental shelf caused by tidal mixing and runoff from the continent. Modeling studies have suggested that the Antarctic Peninsula is a feasible source for the large krill populations found near South Georgia in the Southern Ocean (Hofmann *et al.* 1998).

Ventilation of the deep ocean and nutrient supply into the Antarctic Circumpolar Current both require exchanges between shelf waters and water masses associated with much greater depths. However, the major currents around the margins of Antarctica are thought to be tied to isobaths and are associated with weak cross-slope flows. In particular, the Antarctic Coastal Current and the Antarctic Slope Front may act as barriers to shelf-slope exchange.

The Coastal Current and the Slope Front are the major topographically-driven westward currents found along much of the margin of Antarctica. These currents are important for the preconditioning of shelf waters for the formation of Antarctic Bottom Water (Fahrbach *et al.* 1992), for supplying waters beneath ice shelves and for melting the underside of the ice shelf (Fahrbach *et al.* 1994*a*) and for the transport of Antarctic krill and nutrients (Pauly *et al.* 2000). Furthermore, the interaction between these currents and sea ice, ice shelves and shelf water helps control freshwater fluxes around Antarctica, knowledge of which is essential for accurate climate modeling. Locations where transport across these fronts occurs and the physical processes that enable this exchange are poorly understood.

The Antarctic Slope Front marks the subsurface boundary between cold, relatively fresh water found on the Antarctic continental shelf and the warmer, more saline water further offshore (Jacobs 1986, 1991). The transition across the Slope Front, which is typically found above or just offshore of the shelf break, is characterized by strong horizontal gradients in temperature and salinity. The physical properties of the Slope Front also have important biological implications, since the region associated with the current has been noted for high plankton production and increased sightings of krill predators such as sea birds and whales (Ainley and Jacobs 1981, Pauly *et al.* 2000). The Antarctic Coastal Current is a fast, shallow flow over the continental shelf, often associated with the front of the ice shelf. The Coastal Current is not tied to a particular bathymetric feature and in regions where the shelf is narrow the Coastal Current and the Slope Front may merge (Heywood *et al.* 1998). The Coastal Current and Slope Front then separate and become distinct features where the shelf broadens again.

The Coastal Current and Slope Front are nearly circumpolar, however, they undergo important modifications near the tip of the Antarctic Peninsula due to the influence of complex topographical features and the confluence of these currents with the more rapidly flowing Antarctic Circumpolar Current. The latter is most apparent on the western side of the Peninsula, where Circumpolar Deep Water, typically found offshore of the shelf break, flows up onto the continental shelf and prohibits the formation of the Slope Front (Whitworth *et al.* 1998). The role of complex topography to the north and east of the tip of the Peninsula, especially on flows in Bransfield Strait and along the South Scotia Ridge, muddies the traditional definitions of the Slope Front. In particular, Whitworth *et al.* (1998) suggested that the shoreward extent of the 0°C isotherm, the marker of the Slope Front proposed by Jacobs (1991), does not consistently correspond to the current's position in this area.

Heywood *et al.* (2004) explored the fate of the Coastal Current and Slope Front to the northeast of the Antarctic Peninsula and provided the first maps of these currents near the Peninsula's tip. A distinct Coastal Current was detected over the continental shelf to the east of Joinville Island (Figure 1). Here the Coastal Current is not tied to a particular isobath and flows westward into Bransfield Strait. The Slope Front, which appears as a single core of northward flow east of Bransfield Strait, splits into two features north of Powell Basin. The shoreward portion is tied to isobaths around 1000 m and crosses the South Scotia Ridge, while the portion tied to deeper isobaths becomes the Weddell Front, which is tied to isobaths between 2500 and 3000 m south of the South Orkney Plateau.

A number of questions remain about the behavior of the Coastal Current and Slope Front northeast of the Antarctic Peninsula. The fate of the Coastal Current after it enters Bransfield Strait could not be assessed from the hydrographic data available to Heywood *et al.* (2004). If the Coastal Current continues westward beyond Bransfield Strait and is truly circumpolar, this feature may provide a mechanism for supporting a westward propagating wavelike anomaly pattern observed in ice-ocean models (Beckmann and Timmermann 2001). Furthermore, a number of the hydrographic stations used by Heywood *et al.* (2004) were aligned along the continental slope rather than across it, making it difficult to assess the structure of the Slope Front and the degree to which this current is tied to a particular isobath.

A comprehensive study of the currents and fronts near the tip of the Antarctic Peninsula is the aim of the Antarctic Drifter Experiment: Links to Isobaths and Ecosystems (ADELIE) project. Data for this project were obtained during a research cruise off the tip of the Antarctic Peninsula, crossing the continental shelf and slope into the Weddell Sea (Figure 1). Lagrangian data obtained from surface drifters and Argo floats tracked the paths of the Slope Front and Coastal Current, while a high resolution hydrographic section was used to identify the location and transport of the fronts near the drifter deployment locations. Specific goals of the ADELIE project are to determine the extent to which frontal currents are tied to isobaths in this region and to map possible pathways for Antarctic krill and nutrients near the Antarctic Peninsula. Here we consider the results of the hydrographic section in order to determine the magnitude of the transport associated with the fronts, to assess the physical processes that contribute to the structure of the fronts and to understand how these processes influence cross-slope exchange in the western Weddell gyre.

Many physical processes occurring near the shelf break may contribute to shelf-slope exchanges, but it is still unclear how these different dynamics acting in concert hinder or facilitate exchange. A basic characteristic of water around the margin of Antarctica, and especially in the western Weddell sea, is its weak stratification. This aids topographic control of the flow such that currents tend to follow contours of f/H. However, topographically-steered jets are often associated with strong lateral shears that can develop into unstable frontal waves (Lozier *et al.* 2002). Other mechanisms that can generate eddies and meanders that enhance cross-slope flows are baroclinic instability over the continental slope (Tanaka and Akitomo 2001) and flow interaction with rough topographical features such as submarine ridges (Darelius and Wåhlin 2007) and canyons (Baines and Condie 1998). Tidal currents are frequently largest along the shelf break (Padman *et al.* 2002), and this may lead to periodic or episodic bursts of cross-slope flow. Wind-forced near-inertial motion may provide a similar source of cross-slope velocity variance at the shelf break.

We begin by reviewing previous observations of the Slope Front around the Weddell Gyre in section **2**. Section **3** summarizes the data collection methods used during the ADELIE research cruise. The results of the hydrographic section are presented in section **4** and discussed in section **5**. We conclude by summarizing our findings in section **6**.

2 The Antarctic Slope Front around the Weddell Gyre

Sverdrup (1953) originally argued that the Slope Front arises from the predominantly westerly winds around the margins of Antarctica, which drive an onshore Ekman flow that sets up a westward geostrophic current. Gill (1973) first described how dense water on the shelf that escapes and cascades down the continental slope could play an important role in the formation and localization of the Slope Front. Recently, Baines (personal communication) has expanded on Gill's model and shown that entrainment into a dense, turbulent plume can destabilize the water column on the shoreward side of the Slope Front. The resulting overturning is cited as an important process in the formation of the V-structure associated with the Slope Front (Jacobs 1991).

While the Slope Front is nearly circumpolar, the degree of baroclinicity of the current, the strength and number of cores and the presence of the V-structure in isotherms and isohalines may all vary. The V-structure is an indication of mixing between dense Shelf Water and Modified Warm Deep Water near the continental shelf break (Gill 1973, Foster and Carmack 1976). In regions where mixing of this type does not occur, isopycnals dip downward toward the shore across the Slope Front (Heywood *et al.* 1998). Changes in the structure of the Slope Front around Antarctica, and even the Weddell Gyre, suggest that the physical processes driving the current evolve as the flow propagates westward.

In the eastern Weddell Sea, the Slope Front splits into two cores above the continental slope, centered along isobaths of 1000 m and 3000 m respectively (Heywood *et al.* 1998). The Slope Front has a large barotropic component with surface currents in the southern (shoreward) core on the order of 50 cm s^{-1}. However, the flow also has an important baroclinic character in the southern core, which includes a region of weak undercurrent back to the east. The deeper northern core, on the other hand, is predominantly barotropic. In the eastern Weddell Sea, the continental shelf is narrow, and Heywood *et al.* (1998) do not observe the Coastal Current as a separate flow, although there is evidence that this feature has merged with the Slope Front. Also, because of the narrow shelf, the southeastern Weddell Sea is not a region of bottom water production (Fahrbach *et al.* 1994*a*), and therefore the V-structure is absent in Heywood *et al.*'s (1998) vertical section of potential temperature and salinity.

Further downstream in the gyre, Whitworth *et al.* (1998) display a section at 35°W, just to the west of the Filchner Depression. Here, the temperature and salinity fields display a V-shaped front above the shelf break between 200 m and 600 m depth. This section only samples to a depth of 2000 m, so it is difficult to assess how many velocity cores occur here. Potential temperature values are less than -1°C above the sea bed, but only small isolated regions above the slope have salinity values characteristic of shelf waters. Along the western rim of the Weddell Gyre, Ice Station Weddell (Muench and Gordon 1995) occupied four transects across the continental slope between 65°S and 70°S (all centered at 55°W). Here, tongues of relatively cold and fresh water occupy the entire slope suggesting that dense bottom water with sources further south is actively flowing down or along the slope. The V-structure is easily identified in these sections. The velocity profiles are best resolved in transects 2 (69°S) and

3 (68°S). Both sections have important baroclinic components, however, unlike in the eastern Weddell Sea, the largest velocities are now found at the sea bed rather than at the surface. Along transect 3, there are two distinct northward flowing cores, the first centered over the shelf break and the second over the 2500 m isobath (corresponding with a deeper break in the continental slope). Also, the strongest baroclinic flows are no longer located in the cores of the front, but rather in the region between the fronts. Frontal structures are more difficult to identify in transect 2, which only sampled to the 2500 m isobath.

In the northwestern Weddell Gyre along the South Scotia Ridge, the V-structure across the Slope Front no longer appears (Heywood *et al.* 2004). This absence of a V-structure suggests that the ADELIE section is one of the last locations around the Weddell Gyre where bottom water plays an active role in the formation of the Slope Front. Where water is exported across the South Scotia Ridge, it has been hypothesized that the Slope Front splits to form a new front associated with deeper isobaths, the Weddell Front (Heywood *et al.* 2004).

Thus, around the Weddell Gyre the Slope Front transitions from a surface-intensified flow to a bottom-intensified flow facilitated by the deep outflow of Weddell Sea Bottom Water. Furthermore, the Slope Front is often described as having a two-core structure, approximately centered over the 1000 m and 3000 m isobaths.

3 Data collection

We present hydrographic observations and current measurements obtained on the Antarctic continental shelf and slope of the western Weddell Sea during ADELIE, Cruise 158 of RRS *James Clark Ross* (JCR), in February 2007 (Figure 1). Beginning near Joinville Island at the tip of the Antarctic Peninsula, the JCR steamed southeast along the WOCE repeat line SR04 deploying 40 surface drifters until reaching a depth of approximately 4100 m. The location of the final drifter deployment—also the location of the first hydrographic station—was roughly 400 km from the tip of the Peninsula. The ship then returned along the same section occupying 19 full-depth hydrographic stations and releasing four Argo floats. The final hydrographic station was taken in the same location as a test station at the start of the cruise. A third crossing of the section was completed out to the 2000 m isobath to obtain a clean shipboard acoustic Doppler current profiler (ADCP) section. In this paper we discuss the data collected along the

ADELIE hydrographic section. Discussion of data obtained from the Lagrangian surface drifters will appear in a separate study.

Hydrographic stations were undertaken using a Sea-Bird conductivity-temperature-depth (CTD) sensor along with a SBE-35 Deep Ocean Standards Thermometer and a SBE-43 Oxygen Sensor. A downward looking 300 kHz RDI Workhorse lowered ADCP was used to obtain current measurements at each of the CTD stations. The CTD sensor and LADCP were hosted on a 12-way rosette. Only eight bottles were fitted on the rosette to accompany an upward-looking LADCP, which requires four bottle positions. Unfortunately, the second LADCP was not replaced in time for the cruise following an earlier malfunction. The remaining LADCP was chosen to be deployed in a downward-looking configuration to enable bottom tracking.

Station spacing was close over the shelf break and steep topography (less than 10 km) and widened out towards the central Weddell Sea (Figure 1). The mean station spacing for the section was 20 km. Accuracies were 0.001°C for temperature and 0.002 for salinity. The salinities were calibrated using IAPSO standard seawater (batch 144). Further details of the precision and accuracy of measurements during the cruise are discussed in the cruise report (Thompson 2007).

The LADCP data were processed using Lamont Doherty Earth Observatory (LDEO) software, v. 10.0 (Visbeck, 2002). Stations 9 through 20 were completed with a three beam solution due to a failure in beam four of the LADCP. At each station the up and down casts of the LADCP were averaged and then rotated to yield the component of current perpendicular to the line between each station pair. A 75 kHz RD Instruments Ocean Surveyor (OS75) ADCP installed on the JCR was used to acquire current measurements up to a depth of 700 m throughout the cruise. The agreement between LDEO velocities and those recorded by the shipboard ADCP is excellent.

The section was completely free from sea ice throughout the ADELIE cruise, although sea ice formation was well underway approximately 100 km further south in the Weddell Sea. Observations from the AMSR-E Sea Ice maps from the University of Bremen (Spreen *et al.* 2005) indicate that active sea ice formation over the continental shelf and shelf break along the ADELIE section began to occur approximately 25 days after occupation of the hydrographic section.

4 Results

4.1 Water masses

Figures 2 through 5 show vertical sections of potential temperature, salinity, dissolved oxygen and neutral density γ^n. In each of these figures the most striking feature is the V-shaped dip in the contours between stations 12 and 14. This is the well-documented signature of the Antarctic Slope Front. The Slope Front has been defined as a cold, fresh river of water flowing around Antarctica (Gill 1973) and is usually identified by strong subsurface horizontal property gradients (Ainley and Jacobs 1981). The subsurface gradients are indeed strong across the section, e.g. potential temperature changes nearly 1° C in 10 km. A more quantitative definition of the Slope Front is the shoreward extent of the 0°C isotherm (Jacobs 1991), which corresponds to the base of the V in Figure 2. The dashed line labeled ASF marks the core of the Slope Front as determined from the geostrophic velocity measurements (see section **4.2.2**). In the property sections, the position of the core generally corresponds to the region of strong horizontal gradients on the shoreward side of the V.

The clear V-structure confirms that bottom water cascading over the shelf break was active during the ADELIE cruise. The core of the Slope Front is found approximately 25 km offshore of the shelf break (near station 15). This distance is larger than the Rossby deformation radius, $\ell_R \approx 10 - 15$ km, which would allow dense water cascading off the shelf to turn northward under the Coriolis effect. Thus the deep outflow likely plays an important role in determining the location and strength of the Slope Front.

Over the broad continental shelf temperature is well-mixed with values less than -1°C. There is no signature of the Coastal Current in the temperature section. A V-shaped dip in the isohalines coinciding with station 18 (Figure 3) indicates that the Coastal Current is largely driven by salinity anomalies in this region of the Weddell Gyre. Although not traditionally tied to topography, the Coastal Current is located at a sharp change in bathymetry in this section. This bathymetric feature also corresponds with the shoreward edge of a region near the sea bed with a strong horizontal gradient in dissolved oxygen (Figure 4, lower panel). The core of the Coastal Current, as indicated by the dashed line labeled CC, corresponds to regions of strong horizontal gradients in both dissolved oxygen and neutral density (Figure 5).

Over the continental slope, slightly warmer surface layers overlie the cold Winter Water layer that has a temperature minimum of $-1.7°C$ (Figure 2). Moving down through the water column, temperature has a maximum of $0.6°C$ between 500 and 1000 m, while salinity peaks at 34.69 between these same depths. The temperature and salinity maxima mark Warm Deep Water (WDW) (Carmack and Foster 1975*a*)—a type of Circumpolar Deep Water found exclusively in the Weddell Sea. Using definitions from Whitworth *et al.* (1998), WDW has γ^n values between 28.03 and 28.27 (shaded light gray in Figure 5—the units kg m^{-3} are dropped for brevity). WDW is also characterized by a minimum in dissolved oxygen (200 μmol kg^{-1}). At the level of WDW, the slope of the isohalines reverses sign (Figure 3) indicating the potential for a third deeper front between station 5 and 9. The core of this front, referred to here as the Weddell Front, is marked by the dashed line labeled WF.

Below the WDW the water column is characterized by weak stratification with water becoming cooler and fresher through the level of Weddell Sea Deep Water (WSDW). Near the sea bed, the gradient of the vertical profiles of temperature and salinity increases indicating Weddell Sea Bottom Water (WSBW). This is a cold, fresh and oxygen-rich water mass that extends over the entire continental slope with γ^n values greater than 28.4 (shaded dark gray in Figure 5). While isopycnals slope strongly throughout the water column in the Slope Front, the isopycnals passing through the Weddell Front are most steeply sloped near the sea bed, suggesting that the Weddell Front is strongly influenced by the deep outflow.

The distribution of WSBW can be seen more clearly in the lower panels of Figures 2 through 5, where properties are contoured with height in meters above bottom as the ordinate. These plots indicate that WSBW is not a broad homogeneous water mass found along the continental slope. Instead, there are regions where the bottom water pools and then thins. In the bottom distribution panels, the Slope Front tends to mark a transition between regions of weaker (shoreward) and stronger (seaward) vertical gradients. Weakened stratification likely arises from vertical mixing generated by entrainment into a turbulent downslope flow. Furthermore, strong horizontal gradients in the few hundred meters above the bottom suggest that the deep outflow occurs in isolated jets rather than in a broad northward flow (see section **4.2**). A dip in the contours above the bottom at station 4 may separate two different cores of the deep outflow, possibly from different source regions (Gordon 1998). A similar feature is seen in the bottom distribution of potential temperature shown by Fahrbach *et al.* (2001).

Figure 6 shows potential temperature-salinity diagrams for the ADELIE section and indicates the different water masses encountered. Figure 6(a) shows data from all the measurements divided into stations above the continental shelf (light gray), over the shelf break (gray) and over the continental slope (black) as indicated by the inserted map. The solid lines are best fit contours of neutral density[1]. Figure 6(a) shows the distinction between Shelf Water and Antarctic Surface Water (AASW). Both are primarily stratified in salinity, although Shelf Water tends to be warmer without the remnants of Winter Water.

Figure 6(b) shows an expanded view of stations 15 through 12, which are found over the shelf break and pass through the Slope Front. The signature of the Slope Front can be observed as potential temperature falls from $-0.2°$C ($\square$'s) to $-0.5°$C ($\triangle$'s) and then rises again to $0.3°$C ($\circ$'s) along $\gamma^n = 28.15$. This confirms that we have adequately sampled the Slope Front and the sharp temperature gradient across it, while also illustrating the thinness of the feature. Station spacing across the shelf break is less than 10 km, indicating that the Slope Front is no more than 20 km across in this region of the Weddell Sea. A significant quantity of water with characteristics of WSBW ($\gamma^n > 28.4$) is found for the first time at station 14, near the core of the Slope Front, which may indicate a link between bottom water transport on the upper continental shelf and the location of the Slope Front.

Figure 6(c) shows an expanded view of the stations found over the continental slope with the darker symbols indicating positions further offshore. Whitworth *et al.* (1998) defined the transition between WSDW and WSBW to be the $\gamma^n = 28.4$ contour. A more accurate definition for a particular profile, perhaps, is the change in slope towards colder and less saline waters that occurs between the 28.27 and 28.4 γ^n contours. For the deepest stations, the $\gamma^n = 28.4$ contour accurately marks the transition from WSDW to WSBW. However, moving onshore the transition to WSBW occurs at warmer and more saline values. This evolution could occur with a single end member mixing with progressively warmer and more saline WSDW, but the slight curvature of the data in Figure 6(c), where the curves cross the $\gamma^n = 28.4$ contour indicates that multiple sources of dense water are implicated in the creation of bottom water found in the northwestern

[1]Neutral density is a nonlinear function of potential temperature, salinity, depth, latitude and longitude (Jackett and McDougall 1997). On θ-S diagrams, all samples with a specific value of γ^n are not captured with a single curve. The curves in Figure 6 are third order polynomial fits to data collected within the Weddell Sea and the Atlantic sector of the Southern Ocean.

Weddell Sea (Gordon *et al.* 2001).

Heywood *et al.* (2004) show that a clearer distinction of water masses across the Slope Front is achieved by considering dissolved oxygen variations with changes in neutral density (Figure 7). On the seaward side of the Slope Front, there is a distinct minimum in dissolved oxygen at $\gamma^n = 28.2$, which corresponds to the core of WDW. The shoreward side of the front has greater dissolved oxygen indicating more recently ventilated water. In the Heywood *et al.* (2004) study, the Slope Front is always marked by a sharp transition between high and low dissolved oxygen levels, whereas across the ADELIE section there is a steady evolution through the Slope Front from the high shelf levels to the depleted slope levels. This difference is most likely a result of finer station spacing across the Slope Front that better resolves the transition between the water masses. Although, further north dissolved oxygen levels may be modified in water that has circulated through Bransfield Strait (Heywood *et al.* 2004, Zhou *et al.* 2006).

4.2 Transport

4.2.1 Direct measurements

Figure 8 shows the velocity perpendicular to the ADELIE section (approximately along the slope) from the LADCP measurements. Since the LADCP section provides a snapshot of the velocity field, it is important to remove the tidal contribution to the flow. The LADCP profiles were de-tided using the ESR/OSU suite of high latitude barotropic tidal models (Padman *et al.* 2002). We tested both CATS02.01 (medium resolution, $1/4° \times 1/12°$, Antarctic regional model) and AntPen ($\sim$ 2 km high resolution Antarctic Peninsula model). We found that the latter model provides a good representation of the tidal flows as low frequency oscillations in the shipboard ADCP velocity time series are well-correlated with the predicted tide.

Where the depth is greater than 3000 m, the predicted mean tidal speed is less than 2 cm s^{-1} during a four month period between February and May 2007 and thus has little effect on frontal structure at these locations. Tidal velocities increase up the continental slope and peak at the shelf break. Here tidal velocities can exceed 20 cm s^{-1}, and the predicted mean tidal speed is 8 cm s^{-1} for the same February to May time period. During the ADELIE cruise, the tide model shows that most of the tidal velocity is directed across the slope, which is confirmed by the shipboard ADCP data. Thus we believe that the magnitude of the current associated with the Slope Front observed during ADELIE was not strongly affected by tides. To check the influence of tides on the position of the Slope Front, we identified the Slope Front in both the CTD leg and ADCP leg[2] of the cruise (Figure 1). The location of the core of the Slope Front varies by only 2 km in these two crossings, suggesting that tidal effects did not strongly influence the position of the Slope Front. Tidal velocities on the shelf are more likely to influence the position of the weaker Coastal Current. However, in our two clean crossings, the Coastal Current is easily discernible and found in the same location (the two crossings of the Coastal Current were separated by 10 hours).

The LADCP section (Figure 8) shows three strong bands of northward flow that we identify from the shelf across the slope as the Coastal Current, the Slope Front and the Weddell Front. In section **5** we discuss the connection between the deepest front and the Weddell Front observed south of the South Orkney Islands by Heywood *et al.* (2004). Peak velocities across the section that exceed 30 cm s^{-1} are found within the Slope Front. Velocities in the Coastal Current reach 20 cm s^{-1} at the core, while the Weddell Front is somewhat weaker with velocities between 10-15 cm s^{-1} throughout the water column. Over the continental shelf, southward velocities peak at 8 cm s^{-1}, but over the remainder of the section, little flow moves southward. The strongest horizontal gradients in the flow field are associated with the seaward sides of the Slope Front and the Weddell Front, where regions of strong northward flow rapidly transition to weak southward flows.

The lower panel of Figure 8 shows the bottom distribution of the velocity field as determined from bottom-tracked LADCP measurements. All three of the frontal currents extend to the bottom and in each case, the largest velocities occur at or very close to the bottom. As suggested by the hydrographic data, the deep outflow occurs in a series of narrow, localized cores. The Slope Front has two northward-flowing cores, the first centered at a distance of 150 km along the section, while the second is found about 20 km further offshore. The Slope Front is largely barotropic above its shoreward bottom core, while the seaward bottom core is found below the region of weak southward flow, such that the flow here has a large baroclinic component. The deep outflow centered at the Weddell Front also has a baroclinic component with velocities decaying by a factor of two in the 200 m above the bottom.

[2]Unfortunately the Slope Front could not be accurately identified during the drifter leg because of high turbulence in the surface layers due to a storm.

4.2.2 Geostrophy

Contemporaneous LADCP and shipboard ADCP measurements of the total velocity were used to adjust the geostrophic shear determined from hydrography and thus calculate the total geostrophic current. For each station pair, a depth range was selected where the shears in the geostrophic and LADCP profiles agreed. The offset between the vertically-averaged LADCP velocity and the vertically-averaged geostrophic velocity (averaged over the selected depth range in both cases) determined the barotropic current. For most station pairs, the two LADCP profiles were averaged to obtain a single velocity profile used in determining the offset. In cases where the geostrophic shear and the shipboard ADCP shear (between the station pair) agreed closely with only one of the two LADCP profiles, that single LADCP profile was used in determining the offset. This situation occurred in regions with strong horizontal velocity gradients, for example, on the seaward side of the Slope Front. The LADCP profiles were particularly useful in determining the barotropic contribution to the narrow frontal currents.

The derived barotropic currents were added to the geostrophic shears to produce full-depth profiles of the total geostrophic current. Because the largest northward velocities are found near the sea bed, baroclinic velocity profiles referenced to the deepest common level indicate southward transport over most of the section. The total geostrophic flow, however, is almost completely northward (Figure 9). The positions of the three major currents and the magnitudes of their cross-section velocities are largely the same as in the LADCP section (Figure 8). The peak velocity of the Slope Front is 23 cm s^{-1}, compared to 35 cm s^{-1} in the LADCP section. Weak regions of southward flow are still found on the seaward side of the Slope Front and the Weddell Front, although the horizontal gradients of the velocity field are smaller in the geostrophic velocity section.

The main difference between the LADCP and geostrophic velocity sections is in the distribution of the deep outflow. The LADCP section has three distinct cores along the slope, while the geostrophic flow is large above the sea bed throughout the region connecting the Slope Front and the Weddell Front. The deep outflow still peaks at the Slope Front and Weddell Front cores—23 and 18 cm s^{-1} respectively—but it also exceeds 10 cm s^{-1} to a height of nearly 200 m above bottom throughout the area between the these two fronts. The geostrophic section also provides evidence of a fourth deep outflow core between 49°W and 48°W at a depth of nearly

4000 m.

The barotropic component of the flow associated with the fronts has a marked influence on the transport (Figure 10). The thin curve in Figure 10 shows the cumulative volume transport of the *baroclinic* current referenced to the deepest common level. Negative, or southward, transport is indicated by the dashed line. Nearly all of the baroclinic flow is found offshore of the Slope Front and is directed southward. The largest contribution to the baroclinic transport comes from stations between the cores of the Slope Front and Weddell Front and incorporates the region of steepest topography. The total baroclinic transport across the section is -21 Sv, which differs greatly from Heywood *et al.*'s (1998) estimate of 4 Sv of baroclinic transport along the continental slope in the eastern Weddell Sea and the 17 Sv of baroclinic transport in the Weddell Gyre calculated by Whitworth and Nowlin (1987). This result emphasizes the importance of accurately measuring the deep outflow in the western Weddell Sea.

The bold line in Figure 10 shows the total cumulative transport across the ADELIE section referenced to the LADCP data. The total transport to the deepest common level is 41.12 Sv. In the western Weddell Sea, transport in bottom triangles not included in geostrophic calculations can be significant because of the deep outflow. Including the contribution to transport from bottom triangles, as determined by the method described in Appendix **A**, the total transport becomes 45.87 Sv. All subsequent transport estimates reported here include the contribution from bottom triangles. The contributions to the total transport by the Coastal Current, Slope Front and Weddell Front (indicated in Figure 10) are 1.33, 3.89 and 16.79 Sv respectively. Between stations 2 and 4 the greater depth means that a relatively weak northward flow contributes significantly to the total transport across the section.

The main source of uncertainty in the transport estimate is in determining the reference barotropic velocity from the LADCP data. To estimate error bars we apply random barotropic perturbations following a normal distribution with a standard deviation of 2 cm s^{-1} (the characteristic accuracy of the barotropic component of the LADCP flow) to individual velocity profiles. The error is then determined by calculating the rms deviation of 10,000 realizations of the resulting transport. This method gives an uncertainty estimate of 5.55 Sv. Following Gordon *et al.* (2001) a different, 'worst-case' scenario is obtained by assuming that all the LADCP profiles are systematically biased by 1 cm s^{-1} (the instrumental accuracy). In this case the uncertainty is 8.22 Sv. We conclude that the total transport across the ADELIE section is 46 ± 6 Sv. Although the cumulative transport is still increasing between the two deepest stations, Fahrbach *et al.* (1991) estimate that 90% of the total transport of the Weddell Gyre occurs in the western boundary current, thus we believe our transport estimate is close to the total transport in the Weddell Gyre at the time of the observations.

5 Discussion

5.1 Frontal structures

It is well known that in regions of weak stratification, ocean currents are strongly controlled by bottom topography. Fahrbach *et al.* (1994*b*) showed that vertically-averaged current speeds are linearly correlated with the bottom slope, while Fahrbach *et al.* (2001) found that minimum current speeds in the deep outflow layer were generally correlated with a plateau in the continental slope. The frontal currents observed during ADELIE are also influenced by topographical features, but the high resolution of our hydrographic section has indicated a more interesting and complex relationship between bottom topography and the frontal positions.

Figure 11 considers the relationship between slope steepness and different measures of the overlying flow. The steepness of the continental slope is determined from the change in depth between station pairs divided by the distance between the pair. Panel (a) shows the depth-averaged velocity from the total geostrophic velocity field plotted against the bottom slope. There appears to be a weak trend towards increasing velocity with increasing bottom slope up to a value about 0.025, but as the slope increases further, the steepest slopes correspond to some of the weakest velocities along the section. In panel (b) the ratio of the depth-averaged baroclinic transport (referenced to the deepest common level) to the barotropic transport is again plotted against bottom slope on log-log axes. In this case the trend is much clearer with the flow becoming increasing "baroclinic" with increasing bottom slope.

The continental slope may act as a stabilizing mechanism through a topographical β-effect, such that flow paths are constrained to move along isobaths to minimize changes in potential vorticity. On the other hand, the continental slope may destabilize the flow by tilting isopycnals and increasing available potential energy that is released through baroclinic instability. Foldvik *et al.* (1985*b*) and Foster *et al.* (1987) both suggested that baroclinic instability was active in the western Weddell Sea based on observations along the shelf break. Tanaka and Akitomo (2001) considered numerical experiments using a three-dimensional hydrostatic model to explore the role of slope steepness on baroclinic instability and downslope transport of dense water. Their experiments showed that in steep slope cases (comparable to slopes encountered in the western Weddell Sea), the stabilizing effect of the slope is dominant in the finite amplitude state, and vigorous, baroclinic eddies are confined to the shelf break.

Across the ADELIE section, the flow is predominantly barotropic between the shelf break and the Slope Front, suggesting that potential energy has been converted to barotropic kinetic energy to drive the frontal current. Seaward of the Slope Front and the Weddell Front, the flow in the upper part of the water column experiences a rapid reduction in speed or even a reversal, while the deep outflow remains strong. This generates a baroclinic flow over the steepest topography, which may act to stabilize the flow and maintain its baroclinic character. The slope becomes locally less steep around 2700 m, which may allow baroclinic instability to become active again and extract energy stored in the tilted isopycnals to drive the deeper Weddell Front.

The structure of the fronts is tied to the deep outflow as indicated by the V across the Slope Front (Gill 1973). As dense water flows over the shelf, turbulent entrainment into the dense plume causes isopycnals to bend down towards the sea bed. As described above, this isopycnal tilt may drive baroclinic instability or may be stabilized by the continental slope. Thus the lateral shear on the seaward side of the fronts is enhanced at the transition between these two regimes.

The lateral shears generated by the fronts have important implications for mixing and transport in the western Weddell Sea. In particular, strong lateral shears can lead to the growth of unstable frontal waves that may allow cross-slope exchange (Lozier *et al.* 2002). Bower *et al.* (1985) measured the ability of the Gulf Stream to act as a "barrier" or "blender" to transport by contouring water properties against potential density as the ordinate rather than pressure. Producing similar plots of potential temperature, salinity and dissolved oxygen, but using neutral density rather than potential density (Figure 12), strong horizontal gradients along isopycnals greater than $\gamma^n = 28.2$ indicate that the Slope Front acts as a barrier to transport above this level and a blender below. The deeper Weddell Front is associated with much weaker gradients.

Csanady and Hamilton (1988) pointed out that this vertical shift in dynamics is related to the efficiency of vertical mixing along the continental slope. The results of Figure 12 suggest that the role of the Slope Front in cross-slope exchange processes involving the deep outflow and ventilation of the deep ocean may be very different from those involving krill and nutrient transport in near-surface waters.

5.2 The Weddell Front in the western Weddell Sea

Two of the three fronts observed across the ADELIE section, the Coastal Current and the Slope Front, have previously been documented in the western Weddell Sea. The Weddell Front, on the other hand, has not traditionally been recognized as a distinct feature in this location. Two distinct velocity cores were observed over the continental slope in transect 3 of Ice Station Weddell (Muench and Gordon 1995) south of the ADELIE study section. Fahrbach *et al.* (2001) at times observed two separate cores in the deep outflow along SR04 separated by 50 km, although the two deep fronts along the ADELIE section are separated by approximately 100 km. Heywood *et al.* (2004), using DOVETAIL data, detected only the Coastal Current and the Slope Front just to the north of the ADELIE section, but this section, occupied along Joinville Ridge (Figure 1), did not extend as far east as the 3000 m isobath.

Heywood *et al.* (2004) hypothesize that the Weddell Front originates south of the South Orkney Islands from a splitting of the Slope Front. The properties that distinguish the Weddell Front in Heywood *et al.* (2004), a shift in the WDW potential temperature and salinity maxima, also occur between stations 7 and 8 in the ADELIE section (Figure 13). Between these two stations the potential temperature rises nearly 0.1°C and salinity increases by 0.005; these changes are similar to observations made across the South Scotia Ridge during the DOVETAIL study (section K in Heywood *et al.*'s 2004, Figure 1).

Thus we propose that the Weddell Front is an independent feature that may originate in the Southern Weddell Sea, but at least exists along the western rim of the Weddell Gyre. The Weddell Front is tied to isobaths between 2500 and 3000 m and is often found over local changes in the steepness of the continental slope. We hypothesize that north of the ADELIE section the Weddell Front is found to the east of Joinville Ridge and follows the border of Powell Basin cyclonically until connecting with the Orkney Plateau. The narrowness of the front means that prior surveys with coarser resolution away from the shelf break may not have appreciated the importance of this feature.

5.3 Transport estimate

Firm values for the transport in the Weddell Gyre have proved difficult to obtain because of the importance of having an accurate method for estimating the barotropic contribution to the geostrophic flow. Early estimates of the transport gave disparate results: 96.9 Sv (Carmack and Foster 1975*b*) from a hydrographic section referenced to short-term current meters; 76 Sv (Gordon *et al.* 1981) for purely wind-driven transport; and 17 Sv (Whitworth and Nowlin 1987) from a hydrographic section along the Greenwich Meridian referenced to a level of no motion. Fahrbach *et al.* (1991) first reported the importance of the barotropic contribution and showed that 50% - 100% of the transport in the Weddell Gyre could be missed by assuming zero velocity at the bottom.

Fahrbach *et al.* (1994*b*) then used over three years of current meter measurements to reference hydrographic data along the SR04 WOCE section from Joinville Island to Kapp Norvegia (the northwestern part of which is coincident with the ADELIE measurements), and deduced a gyre-wide transport of 29.5 ± 9.5 Sv. Of this 90% of the transport was contained in a boundary current that extended 500 km from the shelf break. From data collected during Ice Station Weddell in the western Weddell Sea, Muench and Gordon (1995) deduced a transport of 28 Sv across a section covering the shelf and slope at 67.5°S. However, this section covered less than 200 km of the continental slope—considerably less than the 500 km boundary current cited by Fahrbach *et al.* (1994*b*) and the nearly 300 km section of continental slope surveyed during ADELIE.

The ADELIE transport, 46 ± 6 Sv (Figure 10), is larger than both Fahrbach *et al.*'s (1994*b*) and Muench and Gordon's (1995) transport estimates. The difference between the ADELIE estimate and the transport calculated by Muench and Gordon (1995) may be due to the extended length and greater depths sampled by the ADELIE section, but Fahrbach *et al.*'s (1994*b*) estimate from a larger section remains considerably smaller. Fahrbach *et al.* (1994*b*) noted that a potential source of error for their transport estimate was the insufficient density of the current meter data. The distance between current meters was on the order of 100 km—much greater than the 20 km width of the Slope Front and Weddell Front during the ADELIE cruise. Coarse resolution of the current meter array may make the velocity extrema associated with the fronts difficult to detect, which could lead to a significant underestimate of the barotropic component of the flow.

Full ocean depth velocity measurements in the Weddell Gyre have been rare. The DOVETAIL study provided one of the few LADCP surveys in the western Weddell Sea (Gordon *et al.* 2001). LADCP profiles are ideal both for detecting the barotropic component across narrow frontal features and for obtaining accurate bottom-tracked measurements of the velocity within the deep outflow. Figure 14 shows a geostrophic velocity section where the data are sub-sampled by removing all the odd-numbered stations. The referencing is achieved from the even-numbered LADCP profiles using the same technique described in section **4.2.2**; estimates of transport in bottom triangles are included. While the general features are similar to the full section in Figure 9 (e.g. increased lateral gradients across the Slope Front, a strong deep outflow, increased baroclinicity over the steepest topography), the structure and magnitude of the currents associated with the fronts are lost. The total transport across the section is also reduced to 39 ± 8 Sv.

Of course, a single transect with LADCP referencing only provides a snapshot of the flow field and it is important to assess how representative the LADCP section is of the climatological field. The ADELIE cruise occurred at the end of austral summer when the southern Weddell Sea was in an active stage of sea ice formation, but the northwestern Weddell Sea had experienced a long ice-free period. Muench and Gordon (1995) suggest that the wind-driven Sverdrup transport in the Weddell Gyre peaks at 46 Sv for an open water air-sea drag coefficient and has a minimum transport of 30 Sv in a year-round ice-covered scenario. Thus our transport estimate likely includes a larger wind-driven component than the studies of either Fahrbach *et al.* (1994*b*) or Muench and Gordon (1995), which sampled both ice-covered and open-air periods in the former case and only an ice-covered period in the latter. Furthermore, we encountered a strong storm two days before collecting the hydrographic and LADCP data. This storm could have reduced the already weak stratification over the shelf break and enhanced the flow associated with the Slope Front. Evidence of sea ice formation in the southern Weddell Sea and the property sections presented here indicate that bottom water formation and dense water cascading over the shelf acted to enhance the strength of the Slope Front and possibly the Weddell Front. Fahrbach *et al.* (2001) considered the temporal variability of the deep outflow and found a minimum in transport in December and the maximum in May, thus our sampling of the data does not coincide with a seasonal extremum in transport.

The ability to resolve the strong and narrow frontal currents along with the accurate determination of barotropic currents and deep outflow cores from the LADCP data have offered a new and more complete view of the structure and transport properties of the western Weddell Gyre. These features are the principal reason for arriving at larger transport estimates than previous studies.

6 Summary

We have presented results from a high resolution hydrographic survey to the east of the tip of the Antarctic Peninsula over the continental shelf and slope and into the deep Weddell Sea. We identified three northward-flowing currents that dominate the along-slope flow, the Antarctic Coastal Current, the Antarctic Slope Front and the Weddell Front. These fronts account for less than 20% of the area along the section, but roughly half of the total transport. The total volume transport across the section, 46 Sv, is larger than previous estimates because full-depth LADCP data resolved the narrow frontal currents and accurately determined their associated barotropic velocities. Detection of the previously unreported Weddell Front, found above the 2700 m isobath, partially accounts for the increased transport estimate. We argue that the Weddell Front is the same feature as the strong current found over the 3000 m isobath south of the South Orkney Islands, originally thought to result from a splitting of the Slope Front (Heywood *et al.* 2004).

Results from Lagrangian instruments deployed during the ADELIE cruise should shed further light on the role of physical processes, such as such as extreme wind events and the susceptibility of the flow to baroclinic instability, in determining the frontal structure and in controlling shelf-slope and cross-slope exchanges.

Acknowledgments

We would like to thank all who contributed to the success of the ADELIE research cruise, especially the officers and crew of the RRS *James Clark Ross*. In particular, Nuno Nunes and

Angelika Renner were invaluable in collecting the LADCP and ADCP data during the cruise. We would also like to thank Deb Shoosmith for her assistance in processing the shipboard ADCP data. The cruise was supported by the UK Natural Environment Research Council (NERC) through the Antarctic Funding Initiative, AFI6/25.

A Appendix: Bottom triangle method

Bottom triangles refer to the region below the deepest common level of two adjacent CTD stations where it is not possible to calculate geostrophic velocities directly (Figure 15(a)); the area of this region increases with the distance between stations and the steepness of the continental slope. An accurate method of estimating transport in bottom triangles is particularly important along the slope in the western Weddell Sea where maximum velocities in the water column are typically found at or just above the sea bed.

If we consider station A adjacent to a deeper station B, we begin by calculating the geopotential anomaly ϕ of each station from the hydrographic data[3] (Pond and Pickard 1986). The gradient of ϕ_A at the sea bed is used to linearly extrapolate ϕ_A to the depth of station B (dashed line in Figure 15(a)), such that

$$\phi'_A(z) = \phi_{A|z=d_a} + \frac{\mathrm{d}\phi_A}{\mathrm{d}z}_{|z=d_a}(z - d_a), \quad z < d_a, \tag{1}$$

where z increases upwards and $z = 0$ at the surface. For depths $d_B < z < d_A$, a new geopotential anomaly $\hat{\phi}$ is created at each level through the bottom triangle from a weighted average of ϕ'_A and ϕ_B:

$$\hat{\phi}(z) = \phi'_A(z)\left(\frac{z - d_B}{d_A - d_B}\right) + \phi_B(z)\left(\frac{d_A - z}{d_A - d_B}\right). \tag{2}$$

The geostrophic velocity is given by

$$V_g(z) = \frac{\phi_B - \hat{\phi}}{2\Omega L \sin\varphi}\left(\frac{d_A - d_B}{z - d_B}\right), \quad d_B < z < d_A, \tag{3}$$

where Ω is the Earth's rotation rate, φ is the mean latitude of the station pair and L is the distance between stations. The transport through the bottom triangle is then

$$\mathcal{V} = \int_{d_B}^{d_A} V_g(z)\, L\left(\frac{z - d_B}{d_A - d_B}\right)\mathrm{d}z. \tag{4}$$

The error associated with the linear extrapolation of ϕ_A in (1) increases with depth, but this has a limited effect on the transport since the width of the bottom triangle decreases with depth.

The total transport in the bottom triangles, as calculated by the method described here, is approximately 4.8 Sv. Transport in the bottom triangles is reduced to 3.9 Sv by simply extending the velocity at the deepest common level to the bottom, which is a commonly used method.

[3]The geopotential is typically represented by ϕ and the geopotential anomaly by $\delta\phi$. We drop the δ here to ease notation.

References

Ainley, D. G. and Jacobs, S. S., 1981. Sea-bird affinities for ocean and ice boundaries in the Antarctic. *Deep-Sea Res. A*, **28**, 1173-1185.

Baines, P. G. and Condie, S., 1998. Observations and modelling of Antarctic downslope flows in *Ocean, Ice, and Atmosphere: Interactions at the Antarctic Continental Margin*, edited by S. S. Jacobs and R. F. Weiss, *Ant. Res. Ser.*, **75**, pp 29-49, AGU, Washington, D. C.

Beckmann, A. and Timmermann, R., 2001. Circumpolar influences on the Weddell Sea: Indication of an Antarctic circumpolar coastal wave. *J. Clim.*, **14**, 3785-3792.

Bower, A. S., Rossby, H. T. and Lillibridge, J. L., 1985. The Gulf Stream—Barrier or blender? *J. Phys. Oceanogr.*, **15**, 24-32.

Carmack, E. C., 1977. Water characteristics of the Southern Ocean south of the Polar Front. In *A voyage of discovery*, George Deacon 70th Anniversary Volume, M. Angel, ed., Pergamon Press, Oxford.

Carmack, E. C. and Foster, T. D., 1975*a*. Circulation and distribution of oceanographic properties near the Filchner Ice Shelf. *Deep-Sea Res.*, **22**, 77-90.

Carmack, E. C. and Foster, T. D., 1975*b*. On the flow of water out of the Weddell Sea. *Deep-Sea Res.*, **22**, 711-724.

Csanady, G. T. and Hamilton, P., 1988. Circulation of slopewater. *Cont. Shelf Res.*, **8**, 565-624.

Darelius, E. and Wåhlin, A., 2007. Downward flow of dense water leaning on a submarine ridge. *Deep-Sea Res. I*, **54**, 1173-1188..

Deacon, G. E. R., 1937. The hydrography of the Southern Ocean. *Discovery Reports*, **15**, 124 pp.

Fahrbach, E., Harms, S., Rohardt, G., Schroder, M. and Woodgate, R. A., 2001. Flow of bottom water in the northwestern Weddell Sea. *J. Geophys. Res.*, **106**, 2761-2778.

Fahrbach, E., Knoche, M. and Rohardt, G., 1991. An estimate of water mass transformation in the southern Weddell Sea. *Marine Chem.*, **35,** 25-44.

Fahrbach, E., Peterson, R. G., Rohardt, G., Schlosser, P. and Bayer, R., 1994*a*. Suppression of bottom water formation in the southeastern Weddell Sea. *Deep-Sea Res. I*, **41**, 389-411.

Fahrbach, E., Rohardt, G. and Krause, G., 1992. The Antarctic coastal current in the south-eastern Weddell Sea. *Polar Biol.*, **12**, 171-182.

Fahrbach, E., Rohardt, G., Schroder, M and Strass, V., 1994*b*. Transport and structure of the Weddell Gyre. *Ann. Geophysicae*, **12**, 840-855.

Falkowski, P. G., Barber, R. T. and Smetacek, V., 1998. Biogeochemical controls and feedbacks on ocean primary production. *Science*, **281**, 200-206.

Foldvik, A. and Gammelsrød, T., 1988. Notes on Southern Ocean hydrography, sea-ice and bottom water formation. *Palaeogeography, Palaeoclimatology, Palaeoecology*, **67**, 3-17.

Foldvik, A., Gammelsrød, T. and Tørresen, T., 1985*a*. Circulation and water masses on the southern Weddell Sea shelf, in *Oceanography of the Antarctic Continental Shelf*, S. S. Jacobs, ed. *Antarctic Research Series*, **43**, American Geophysics Union, 5-20.

Foldvik, A., Kvinge, T. and Tørresen, T., 1985*b*. Bottom currents near the continental shelf break in the Weddell Sea in *Oceanography of the Antarctic Continental Shelf*, edited by S. S. Jacobs, *Ant. Res. Ser.*, **43**, pp 21-34, AGU, Washington, D. C.

Foster, T. D. and Carmack E. C., 1976. Frontal zone mixing and Antarctic Bottom Water formation in the southern Weddell Sea. *Deep-Sea Res.*, **23**, 301-317.

Foster, T., D., Foldvik, A. and Middleton, J. H., 1987. Mixing and bottom water formation in the shelf break region of the southern Weddell Sea. *Deep-Sea Res.*, **34**, 1771-1794.

Gill, A. E., 1973. Circulation and bottom water production in the Weddell Sea. *Deep-Sea Res.*, **20**, 111-140.

Gordon, A. L., 1998. Western Weddell Sea thermohaline stratification, in *Ocean, Ice, and Atmosphere: Interactions at the Antarctic Continental Margin*, edited by S. S. Jacobs and R. F. Weiss, *Ant. Res. Ser.*, **75**, pp 215-240, AGU, Washington, D. C.

Gordon, A. L., Martinson, D. G. and Taylor, H. W., 1981. The wind-driven circulation in the Weddell-Enderby Basin. *Deep-Sea Res.*, **28**, 151-163.

Gordon, A. L., Visbeck, M. and Huber, B., 2001. Export of Weddell Sea Deep and Bottom water. *J. Geophys. Res.*, **106**, 9005-9017.

Heywood, K. J., Locarnini, R. A., Frew, R. D., Dennis, P. F. and King, B. A., 1998. Transport and water masses of the Antarctic Slope Front system in the eastern Weddell Sea, in *Ocean, Ice, and Atmosphere: Interactions at the Antarctic Continental Margin*, edited by S. S. Jacobs and R. F. Weiss, *Ant. Res. Ser.*, **75**, pp 203-214, AGU, Washington, D. C.

Heywood, K. J., Naveira Garabato, A. C., Stevens, D. P. and Muench, R. D., 2004. On the fate of the Antarctic Slope Front an dthe origin of the Weddell Front. *J. Geophys. Res.*, **109**, C06021, doi:10.1029/2003JC002053.

Hofmann, E. E., Klinck, J. M., Locarnini, R. A., Fach, B. A. and Murphy, E. J., 1998. Krill transport in the Scotia Sea and environs. *Ant. Sci.*, **10**, 406-415.

Jackett, D. and McDougall, T. J., 1997. A neutral density variable for the world's oceans. *J. Phys. Oceanogr.*, **27**, 237-263.

Jacobs, S. S., 1986. The Antarctic Slope Front. *Antarct. J. U. S.*, **21**, 123-124.

Jacobs, S. S., 1991. On the nature of the Antarctic Slope Front. *Marine Chem.*, **35**, 9-24.

Lozier, M. S., Reed, M. S. C. and Gawarkiewicz, G. G., 2002. Instability of a shelfbreak front. *J. Phys. Oceanogr.*, **32**, 924-944.

Mantyla, A. W. and Reid, J. L., 1983. Abyssal characteristics of the World Ocean waters. *Deep-Sea Res.*, **30**, 805-833.

Middleton, J. H., Foster, T. D., and Foldvik, A., 1987. Diurnal shelf waves in the southern Weddell Sea. *J. Phys. Oceanogr.*, **17**, 784-791.

Muench, R. D. and Gordon, A. L., 1995. Circulation and transport of water along the western Weddell Sea margin. *J. Geophys. Res.*, **100**, 18503-18515.

Orsi, A. H., Smethie, W. M. and Bullister, J. L., 2002. On the total input of Antarctic waters to the deep ocean: A preliminary estimate from chlorofluorocarbon measurements. *J. Geophys. Res.*, **107**, 3122, doi:10.1029/2001JC000976.

Padman, L., Fricker, H. A., Coleman, R., Howard, S. and Erofeeva, S., 2002. A new tidal model for the Antarctic ice shelves and seas. *Ann. Glaciol.*, **34**, 247-254.

Pauly, T., Nicol, S., Higginbottom, I., Hosie, G. and Kitchener, J., 2000. Distribution and abundance of Antarctic krill (Euphausia superba) off East Antarctica (80-150°E) during the Austral summer of 1995/1996. *Deep-Sea Res. II*, **47**, 2465-2488.

Pond, S. and Pickard, G. L., 1986. *Introductory Dynamical Oceanography*, 2nd ed. Pergamon Press, Oxford, 329 pp.

Rintoul, S. R., 1998. On the origin and influence of Adèlie Land Bottom Water, in *Ocean, Ice, and Atmosphere: Interactions at the Antarctic Continental Margin*, edited by S. S. Jacobs and R. F. Weiss, *Ant. Res. Ser.*, **75**, pp 151-171, AGU, Washington, D. C.

Smith, W. H. F. and Sandwell, D. T., 1997. Global sea floor topography from satellite altimetry and shpi depth soundings. *Science*, **277**, 1956-1962.

Spreen, G., Kaleschke, L. and Heygster, G., 2005. Operational sea ice remote sensing with AMSR-E 89 GHz channels. 2005 IEEE International Geoscience and Remote Sensing Symposium Proceedings, *IEEE*, **6**, 4033-4036.

Stommel, H. and Arons, A. B., 1960. On the abyssal circulation of the World Oceans. *Deep-Sea Res.*, **6**, 140-154.

Sverdrup, H. U., 1953. The currents off the coast of Queen Maud Land, *Nor. Geogr. Tidsskr.*, **14**, 239-249.

Tanaka, K. and Akitomo, K., 2001. Baroclinic instability of density current along a sloping bottom and the associated transport process. *J. Geophys. Res.*, **106**, 2621-2638.

Thompson, A. F., 2007. ADELIE cruise report, RRS James Clark Ross cruise 158, 9th February-20th February 2007, *UEA Cruise Report Series No. 9*, University of East Anglia, Norwich, U.K., 86 pp.

Thorpe, S. E., Heywood, K. J., Stevens, D. P. and Brandon, M. A., 2004. Tracking passive drifters in a high resolution ocean model: implications for interannual variability of larval krill transport to South Georgia. *Deep-Sea Res. I*, **51**, 909-920.

Visbeck, M., 2002. Deep velocity profiling using lowered acoustic Doppler current profilers–Bottom track and inverse solutions. *J. Atmos. Oceanic Tech.*, **19**, 794-807.

Weiss, R. F., Oestlund and Craig, H., 1979. Geochemical studies of the Weddell Sea. *Deep-Sea Res.*, **26**, 1093-1120.

Whitworth, T. and Nowlin, W. D., 1987. Water masses and currents of the Southern Ocean at the Greenwich Meridian. *J. Geophys. Res.*, **92**, 6462-6476.

Whitworth, T., Orsi, A. H., Kim, S.-J., Nowlin, W. D. and Locarnini, R. A., 1998. Water masses and mixing neat the Antarctic Slope Front in *Ocean, Ice, and Atmosphere: Interactions at the Antarctic Continental Margin*, edited by S. S. Jacobs and R. F. Weiss, *Ant. Res. Ser.*, **75**, pp 1-27, AGU, Washington, D. C.

Zhou, M., Niiler, P. P., Zhu, Y. and Dorland, R. D., 2006. The western boundary current in the Bransfield Strait, Antarctica. *Deep-Sea Res. I*, *53*, 1244-1252.

Figure Captions

Fig. 1. Bathymetry around the tip of the Antarctic Peninsula (Smith and Sandwell 1997). Contours are every 1000 m as well as the 500 m contour. The shade changes every 2000 m, and land is shaded black. The positions of CTD stations occupied during the ADELIE cruise are given by the black dots; stations 1 and 20 were repeat stations carried out at the same location at the beginning and end of the cruise. Important geographical landmarks are labeled in the upper panel; in the lower panel the positions of the fronts are indicated. CC, ASF and WF are the Antarctic Coastal Current, the Antarctic Slope Front and the Weddell Front respectively.

Fig. 2. Potential temperature section. Contours are -1.5, -1, -0.5, 0 and 0.5°C in the upper and middle panels and every 0.25°C from -1.25 to 0°C in the lower panel. Values between -1 and -0.5°C are shaded. Station locations are given by the white numbers in the middle panel and positions of the bottle samples are indicated by the black dots. The lower panel shows potential temperature contoured against distance along the section and height in meters above the bottom. The dashed lines represent the cores of the Coastal Current (CC), the Antarctic Slope Front (ASF) and the Weddell Front (WF) as discussed in section **4.1**.

Fig. 3. Salinity section. Values between 34.5 and 34.65 are shaded. Otherwise as Figure 2.

Fig. 4. Dissolved oxygen section (μmol kg^{-1}). Values between 260 μmol kg^{-1} and 300 μmol kg^{-1} are shaded. Contour intervals in the upper and middle panels are every 20 μmol kg^{-1} between 200 and 340. In the lower panel contours 250, 270 and 290 μmol kg^{-1} have been added. Otherwise as Figure 2.

Fig. 5. Neutral density γ^n section. The region with $28.03 < \gamma^n < 28.27$ is shaded light gray indicating Warm Deep Water (WDW) and Modified Warm Deep Water (MWDW) and the region with $\gamma^n > 28.4$ is shaded dark gray indicating Weddell Sea Bottom Water (WSBW). The water mass boundaries are as defined by Whitworth *et al.* (1998). Otherwise as Figure 2.

Fig. 6. Water mass characteristics shown in potential temperature-salinity diagrams. Panel (a) shows all measurements divided into stations over the continental shelf (light gray dots, stations 16-20), stations over the shelf break (gray dots, stations 12-15) and stations over the continental slope (black dots, stations 2-11). The position of these stations is shown in the insert

of panel (a). The solid lines are curves of neutral density. Antarctic Surface Water (AASW) and Shelf Water are labeled. Panel (b) shows an expanded view of the stations found over the shelf break. Symbols become darker moving offshore. Modified Warm Deep Water (MWDW) is marked. Panel (c) shows an expanded view of the stations found over the continental shelf with symbols becoming darker moving offshore. The neutral density contours 28.1, 28.27 and 28.4 mark the transition between Warm Deep Water (WDW), Weddell Sea Deep Water (WSDW) and Weddell Sea Bottom Water (WSBW).

Fig. 7. Neutral density γ^n-dissolved oxygen (μmol kg^{-1}) diagram. Stations in light gray, gray and black are found over the shelf, over the shelf break and over the continental slope respectively (see inset in Figure 6a).

Fig. 8. Lowered acoustic Doppler current profiler (LADCP) section of velocities perpendicular to the section. The contour intervals are every 5 cm s^{-1} between -10 and 20 cm s^{-1}. The 30 cm s^{-1} contour is also included. Positive (northward) velocities greater than 10 cm s^{-1} are shaded dark gray while negative (southward) velocities are shaded light gray. The lower panel shows the velocity distribution as a function of height above bottom—the contours and shading are the same. Station labeling is as in Figure 2.

Fig. 9. Total geostrophic velocities (cm s^{-1}) across the ADELIE section. The geostrophic shear is referenced to the absolute velocity as determined from the LADCP measurements. The contours are every 5 cm s^{-1} between -5 and 20 cm s^{-1}. Otherwise as Figure 8.

Fig. 10. Cumulative volume transport across the ADELIE section. Open circles denote geostrophic transport relative to zero velocity at the deepest common level of each station pair. Solid circles denote total geostrophic transport, where LADCP measurements were used to determine the barotropic component. Positive (northward) transport is indicated by a solid line, while negative (southward) transport is indicated by a dashed line. The bathymetry of the Antarctic shelf and slope is shown in black and the station numbers are indicated in white. Transport contributions from the Antarctic Coastal Current (CC), Antarctic Slope Front (ASF) and the Weddell Front (WF) are given. The horizontal bar indicates the stations over which these transports were calculated. The gray shaded region marks the cores of the frontal currents where the depth-averaged total geostrophic velocity exceeds 10 cm s^{-1}.

Fig. 11. (*a*) Depth-averaged total geostrophic velocity plotted against steepness of the bottom topography. Open symbols indicate station pairs over the continental shelf, while solid symbols indicate stations pairs over the shelf break and continental slope. Positive slope indicates increasing depth with distance from shore. (*b*) Absolute value of the ratio of the depth-averaged geostrophic velocity, referenced to zero velocity at the deepest common level of each station pair, to the depth-averaged total geostrophic velocity, referenced to the LADCP data, plotted against steepness of the bottom topography.

Fig. 12. (*a*) Potential temperature (°C), (*b*) salinity and (*c*) dissolved oxygen (μmol kg^{-1}) along the ADELIE section contoured against neutral density γ^n as the ordinate. The contour intervals are 0.25°C and 10 μmol kg^{-1} in panels (*a*) and (*c*) respectively; in panel (*b*) contour intervals are 0.2 between 33.4 and 34.4 and 0.025 between 34.5 and 34.7. The dotted lines indicate the locations of the CTD profiles, and the dashed lines indicate the cores of the Antarctic Coastal Current (CC), the Antarctic Slope Front (ASF) and the Weddell Front (WF) as discussed in section **4.1**. Note the change in scale along the ordinate for $27 < \gamma^n < 28$.

Fig. 13. Potential temperature-salinity diagram near the WDW maxima. Properties in gray (black) are found shoreward (seaward) of the Weddell Front.

Fig. 14. Sub-sampled total geostrophic velocities (cm s^{-1}) across the ADELIE section using only data from even-numbered stations. The geostrophic shear is referenced to the absolute velocity as determined from the LADCP measurements. The contours are every 2.5 cm s^{-1} between 2.5 and 10 cm s^{-1}. Otherwise as Figure 8.

Fig. 15. (*a*) Diagram depicting the method of bottom triangles as described in Appendix **A**. The sea bed is shaded black and the bottom triangle region is shaded light gray. The dotted lines indicate the positions of adjacent hydrographic stations A and B. The curves show profiles of geopotential anomaly ϕ (centered on their longitude position). The white dashed line ϕ'_A is a linear extrapolation of the ϕ_A curve to the depth of station B. The velocity across the horizontal level marked by the dashed-dotted line is calculated from the geopotential anomalies $\hat{\phi}$ and ϕ_B (see Appendix **A**). Panels (*b*) through (*e*) show examples from four station pairs of total geostrophic velocities above the deepest common level (black curves) along with the velocity estimates through the bottom triangles (gray curves).

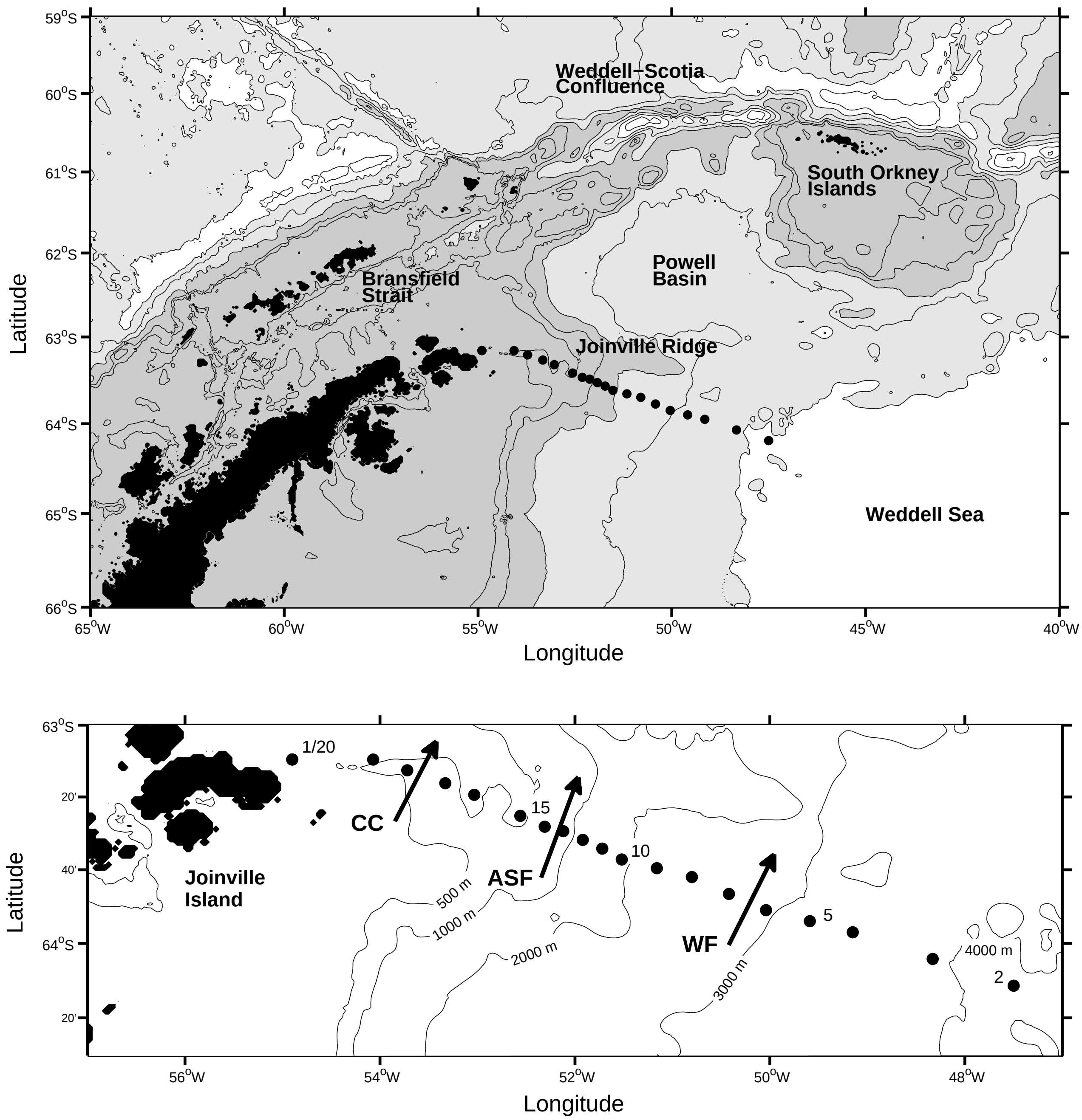

Figure 1: Bathymetry around the tip of the Antarctic Peninsula (Smith and Sandwell 1997). Contours are every 1000 m as well as the 500 m contour. The shade changes every 2000 m, and land is shaded black. The positions of CTD stations occupied during the ADELIE cruise are given by the black dots; stations 1 and 20 were repeat stations carried out at the same location at the beginning and end of the cruise. Important geographical landmarks are labeled in the upper panel; in the lower panel the positions of the fronts are indicated. CC, ASF and WF are the Antarctic Coastal Current, the Antarctic Slope Front and the Weddell Front respectively.

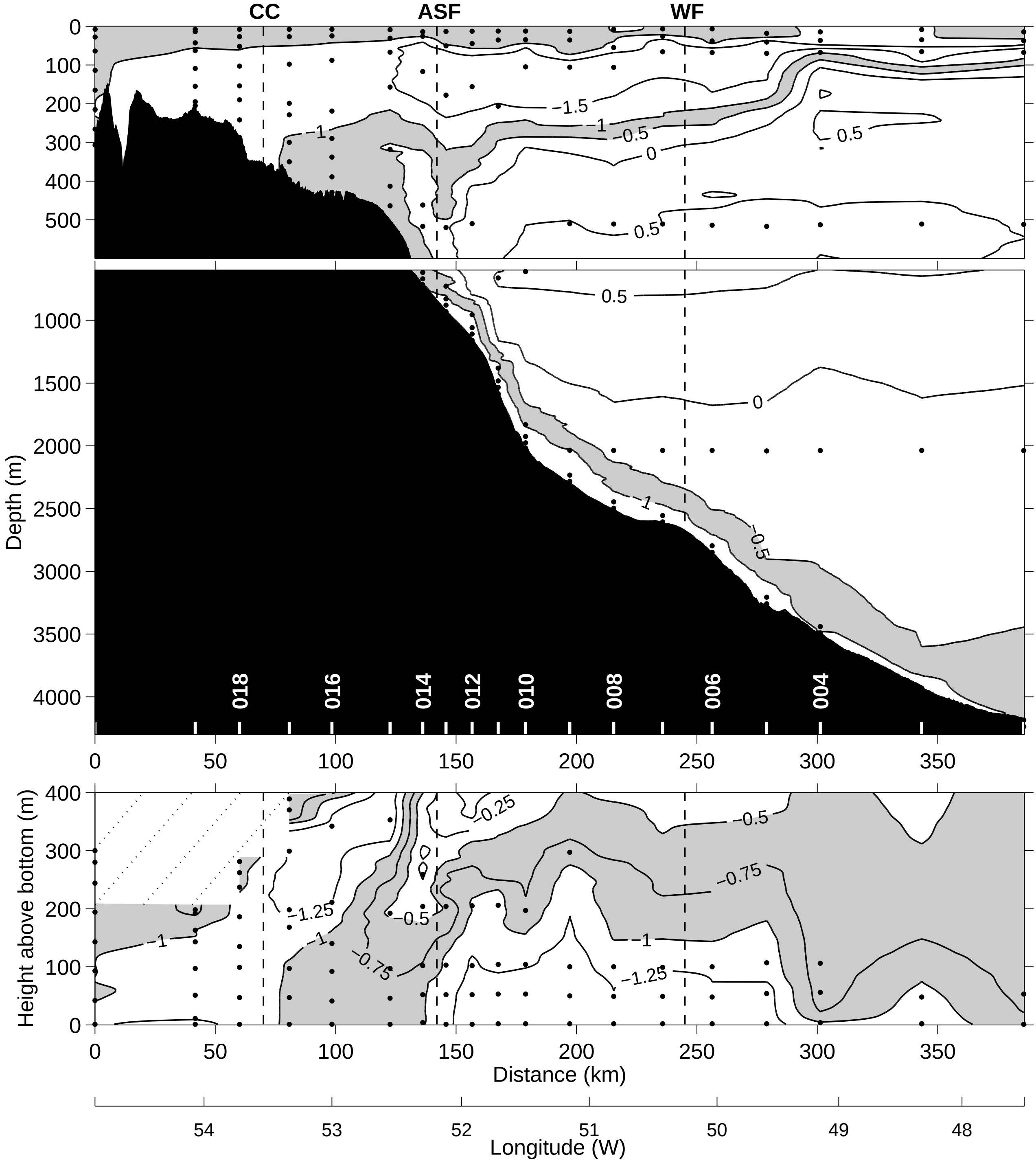

Figure 2: Potential temperature section. Contours are -1.5, -1, -0.5, 0 and 0.5°C in the upper and middle panels and every 0.25°C from -1.25 to 0°C in the lower panel. Values between -1 and -0.5°C are shaded. Station locations are given by the white numbers in the middle panel and positions of the bottle samples are indicated by the black dots. The lower panel shows potential temperature contoured against distance along the section and height in meters above the bottom. The dashed lines represent the cores of the Coastal Current (CC), the Antarctic Slope Front (ASF) and the Weddell Front (WF) as discussed in section **4.1**.

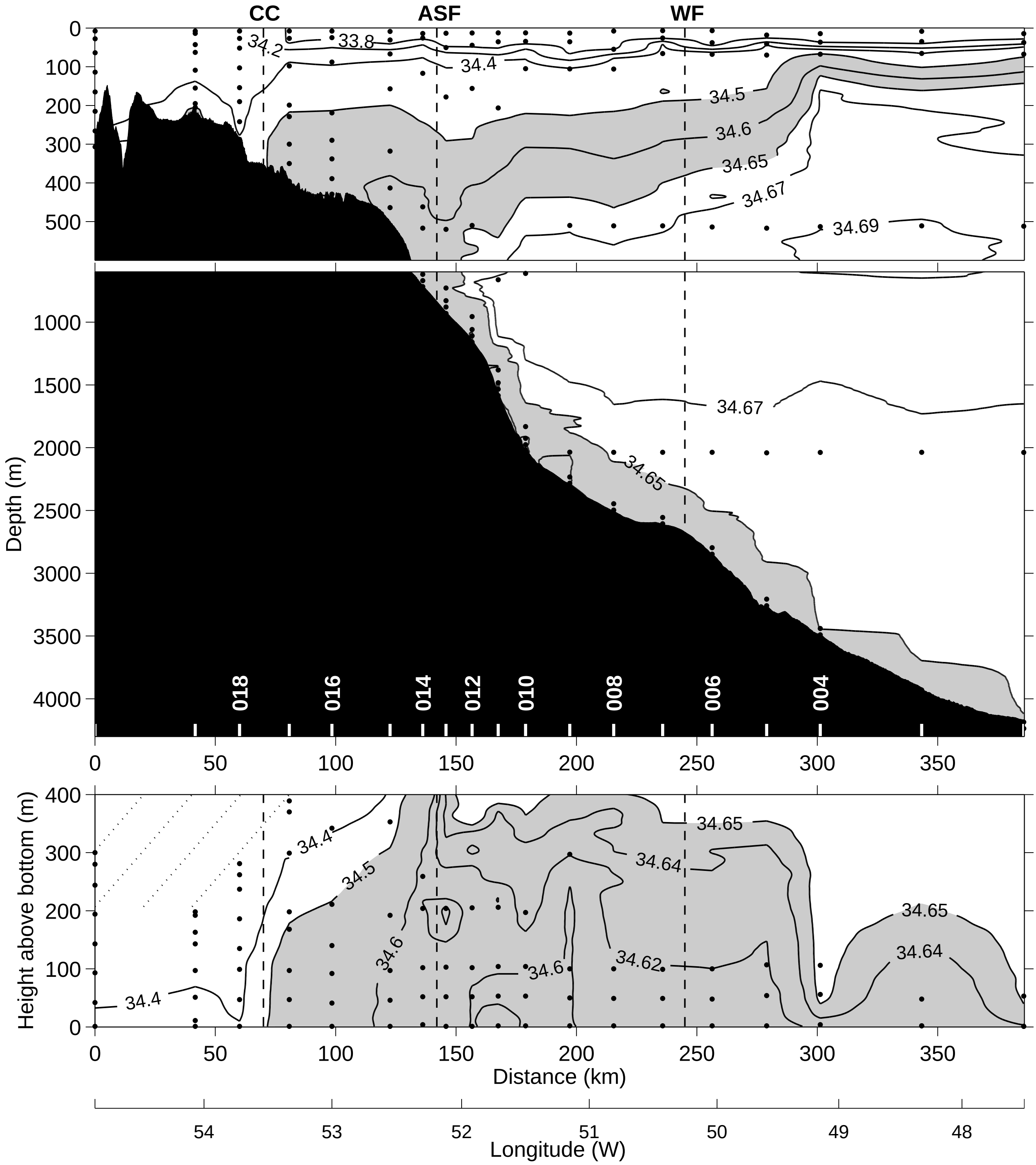

Figure 3: Salinity section. Values between 34.5 and 34.65 are shaded. Otherwise as Figure 2.

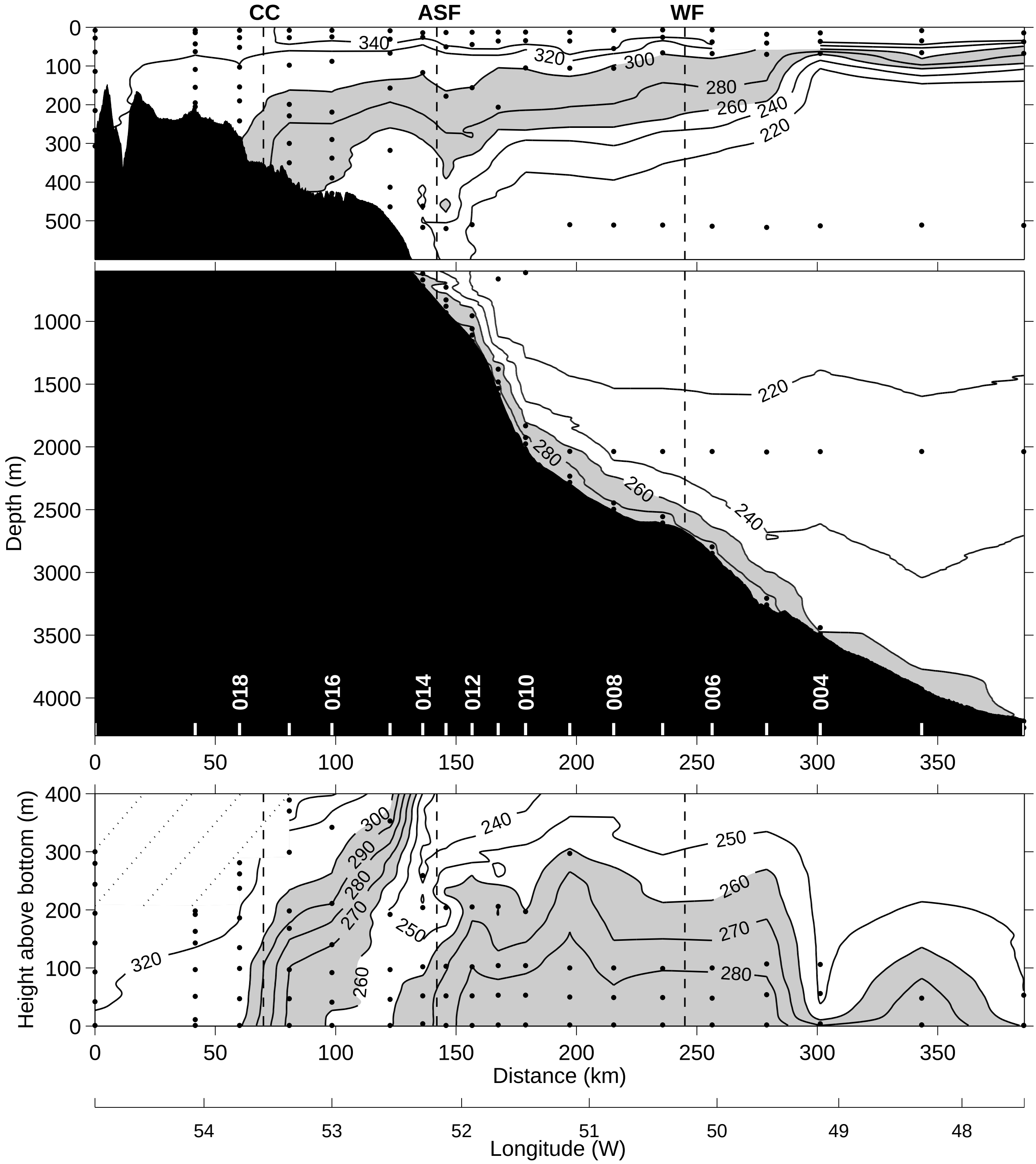

Figure 4: Dissolved oxygen section (μmol kg^{-1}). Values between 260 μmol kg^{-1} and 300 μmol kg^{-1} are shaded. Contour intervals in the upper and middle panels are every 20 μmol kg^{-1} between 200 and 340. In the lower panel contours 250, 270 and 290 μmol kg^{-1} have been added. Otherwise as Figure 2.

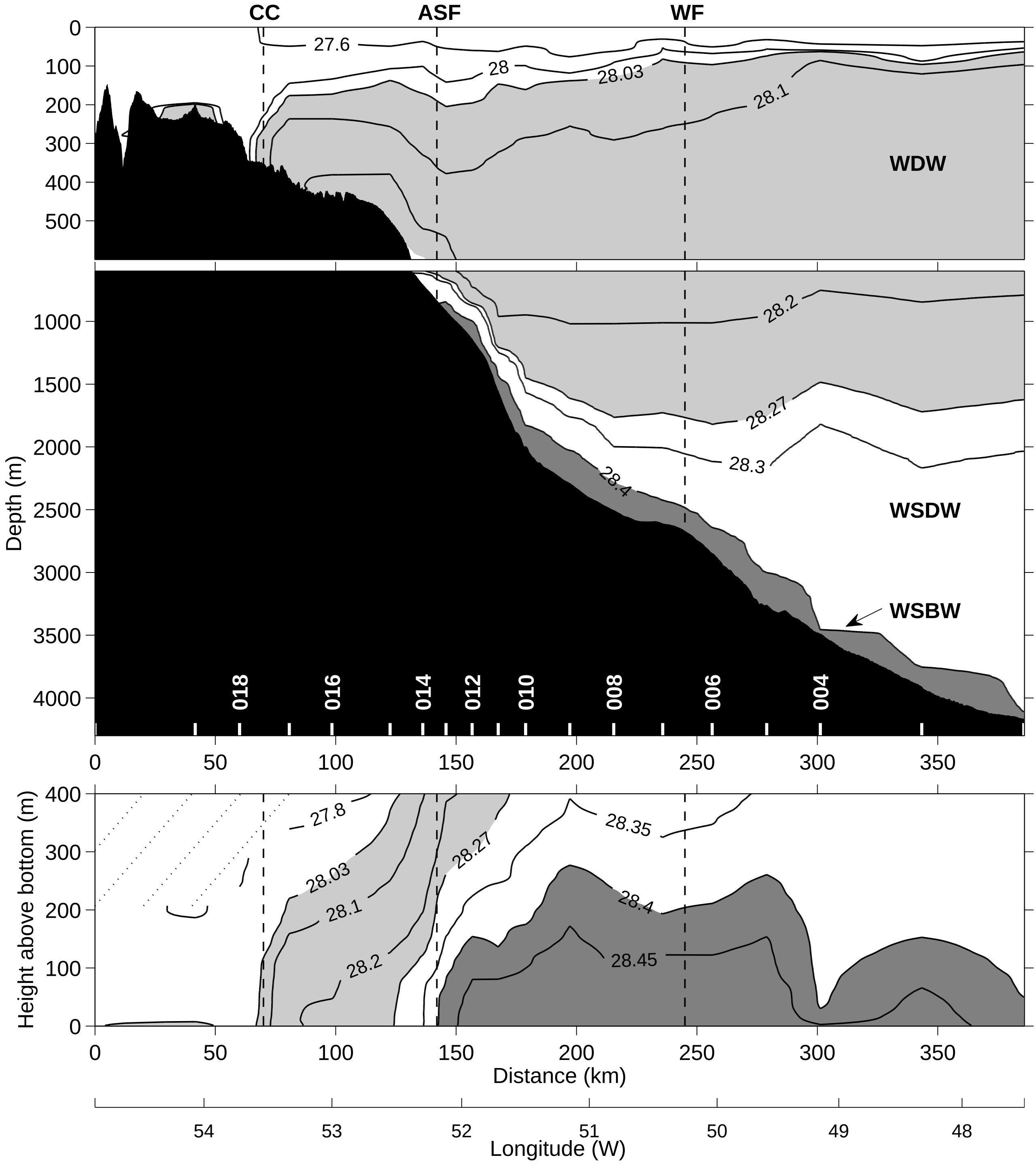

Figure 5: Neutral density γ^n section. The region with $28.03 < \gamma^n < 28.27$ is shaded light gray indicating Warm Deep Water (WDW) and Modified Warm Deep Water (MWDW) and the region with $\gamma^n > 28.4$ is shaded dark gray indicating Weddell Sea Bottom Water (WSBW). The water mass boundaries are as defined by Whitworth *et al.* (1998). Otherwise as Figure 2.

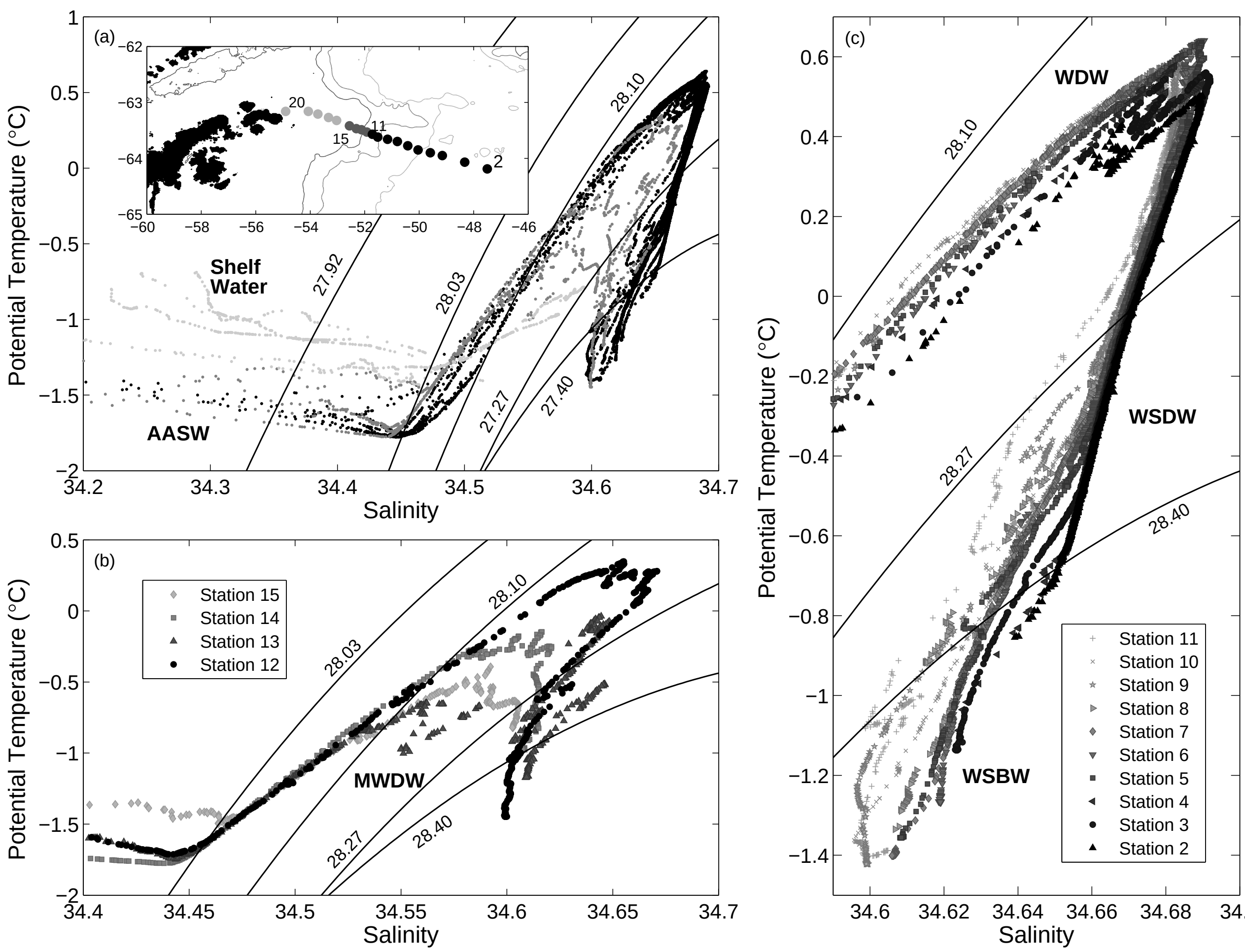

Figure 6: Water mass characteristics shown in potential temperature-salinity diagrams. Panel (a) shows all measurements divided into stations over the continental shelf (light gray dots, stations 16-20), stations over the shelf break (gray dots, stations 12-15) and stations over the continental slope (black dots, stations 2-11). The position of these stations is shown in the insert of panel (a). The solid lines are curves of neutral density. Antarctic Surface Water (AASW) and Shelf Water are labeled. Panel (b) shows an expanded view of the stations found over the shelf break. Symbols become darker moving offshore. Modified Warm Deep Water (MWDW) is marked. Panel (c) shows an expanded view of the stations found over the continental shelf with symbols becoming darker moving offshore. The neutral density contours 28.1, 28.27 and 28.4 mark the transition between Warm Deep Water (WDW), Weddell Sea Deep Water (WSDW) and Weddell Sea Bottom Water (WSBW).

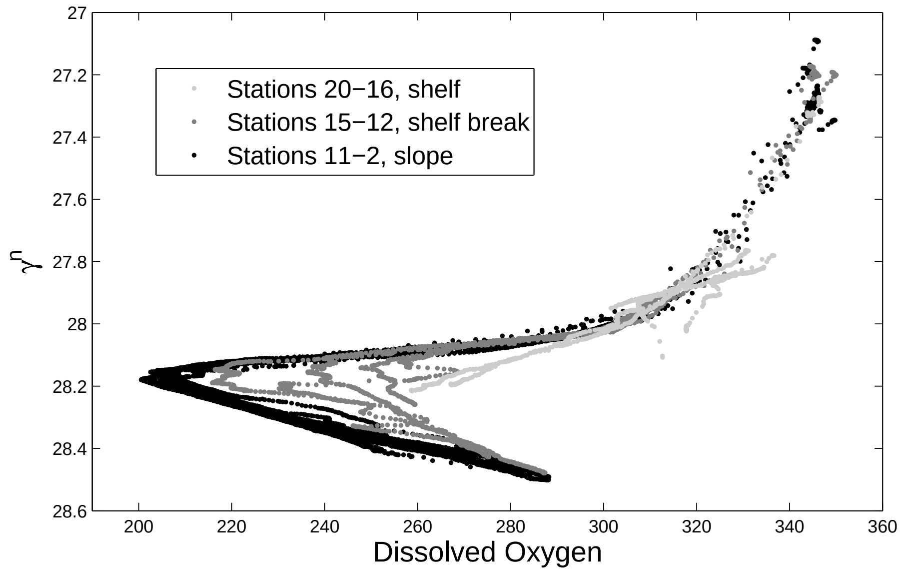

Figure 7: Neutral density γ^n-dissolved oxygen (μmol kg^{-1}) diagram. Stations in light gray, gray and black are found over the shelf, over the shelf break and over the continental slope respectively (see inset in Figure 6a).

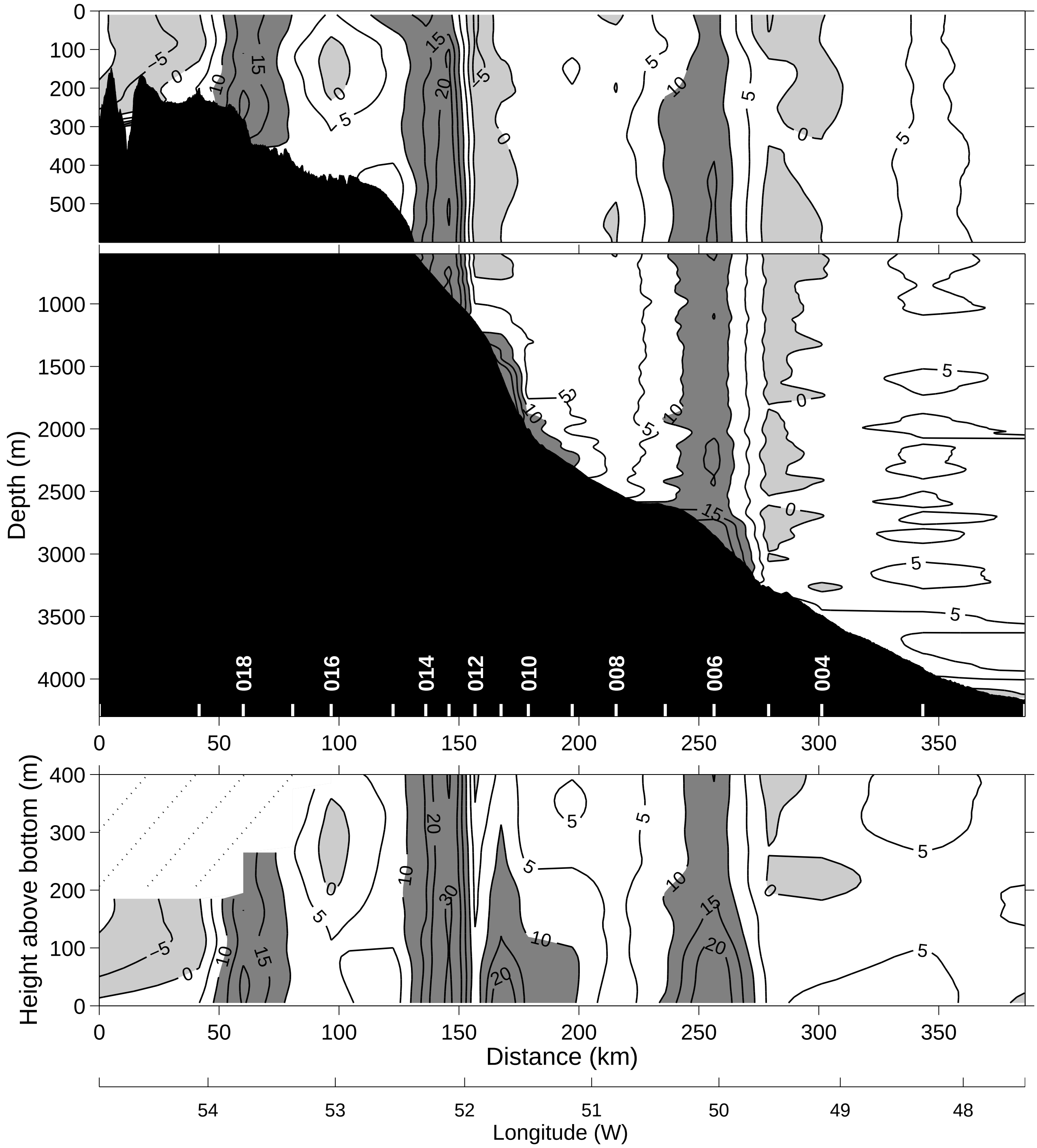

Figure 8: Lowered acoustic Doppler current profiler (LADCP) section of velocities perpendicular to the section. The contour intervals are every 5 cm s^{-1} between -10 and 20 cm s^{-1}. The 30 cm s^{-1} contour is also included. Positive (northward) velocities greater than 10 cm s^{-1} are shaded dark gray while negative (southward) velocities are shaded light gray. The lower panel shows the velocity distribution as a function of height above bottom—the contours and shading are the same. Station labeling is as in Figure 2.

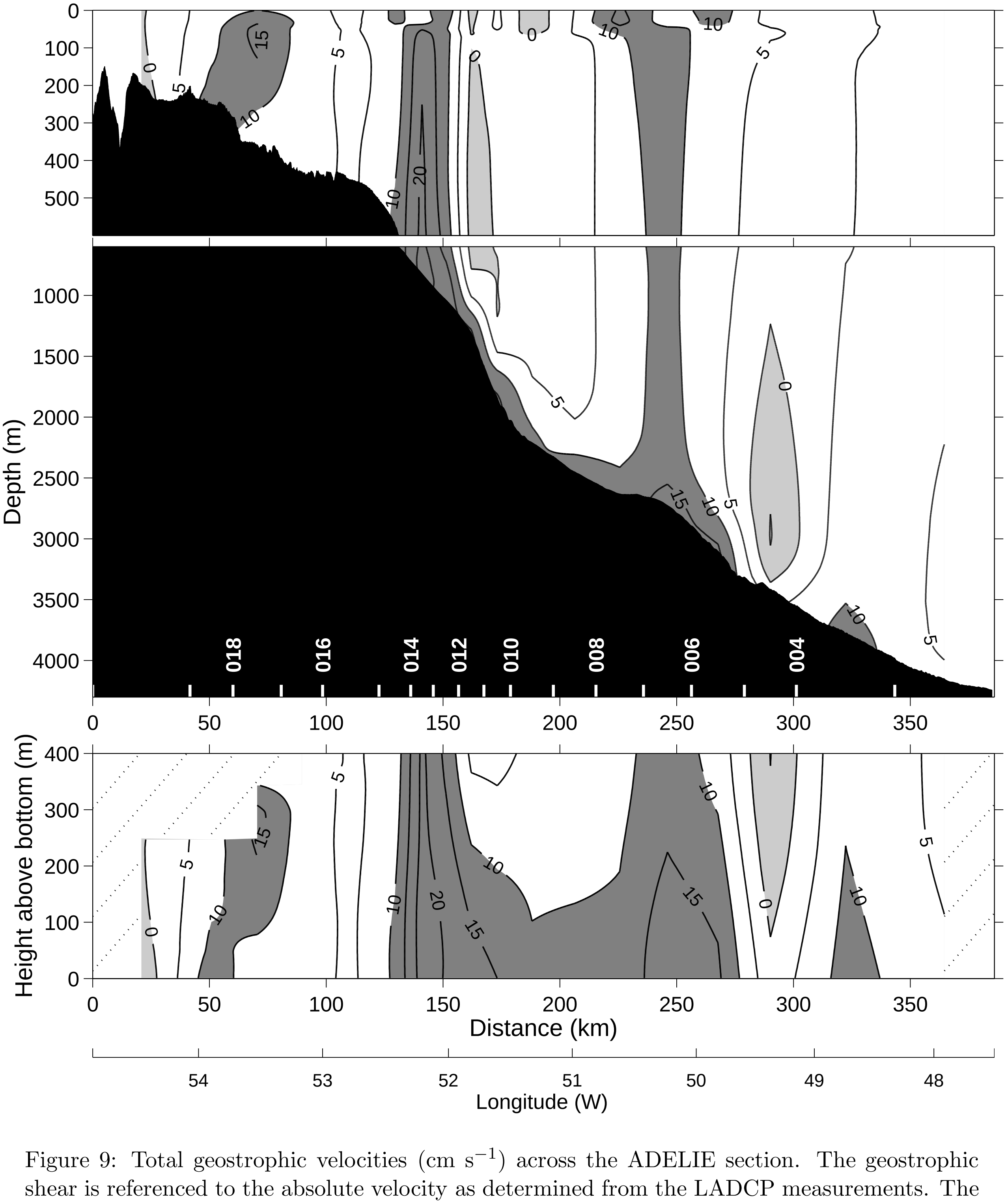

Figure 9: Total geostrophic velocities (cm s^{-1}) across the ADELIE section. The geostrophic shear is referenced to the absolute velocity as determined from the LADCP measurements. The contours are every 5 cm s^{-1} between -5 and 20 cm s^{-1}. Otherwise as Figure 8.

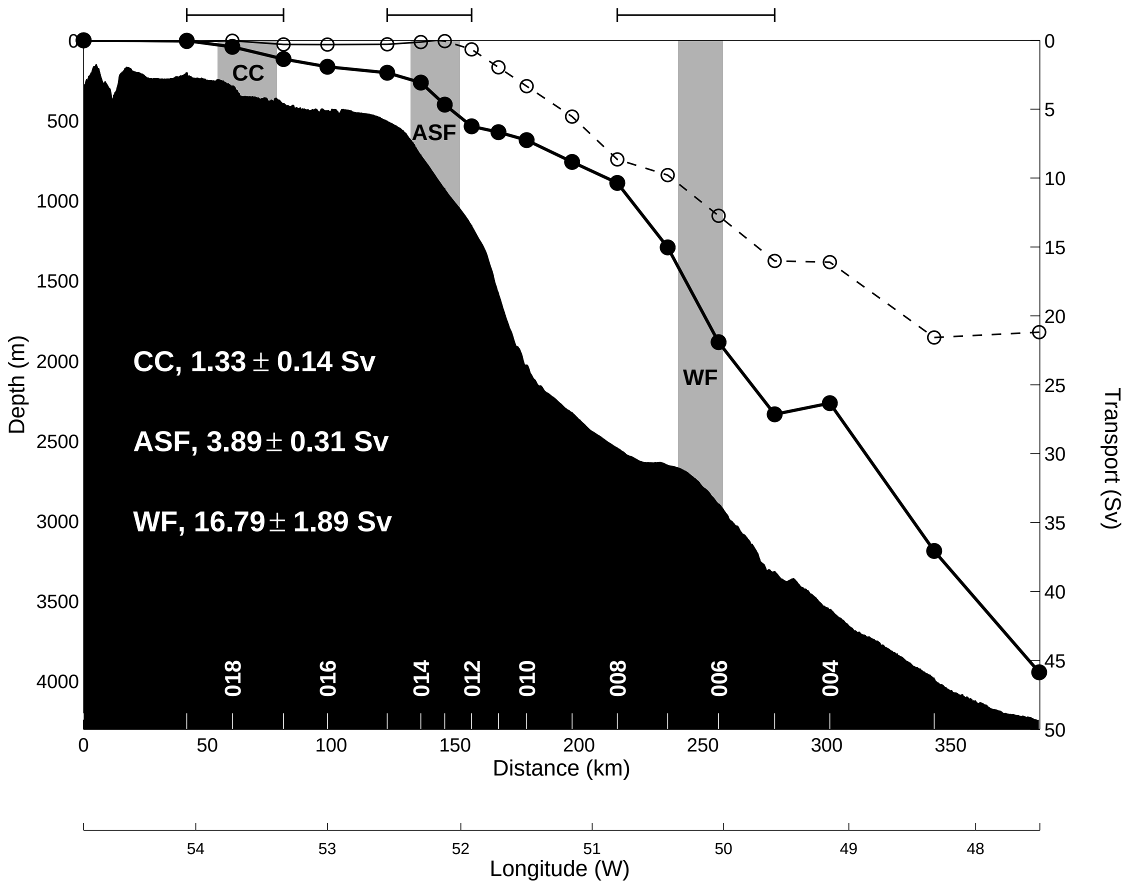

Figure 10: Cumulative volume transport across the ADELIE section. Open circles denote geostrophic transport relative to zero velocity at the deepest common level of each station pair. Solid circles denote total geostrophic transport, where LADCP measurements were used to determine the barotropic component. Positive (northward) transport is indicated by a solid line, while negative (southward) transport is indicated by a dashed line. The bathymetry of the Antarctic shelf and slope is shown in black and the station numbers are indicated in white. Transport contributions from the Antarctic Coastal Current (CC), Antarctic Slope Front (ASF) and the Weddell Front (WF) are given. The horizontal bar indicates the stations over which these transports were calculated. The gray shaded region marks the cores of the frontal currents where the depth-averaged total geostrophic velocity exceeds 10 cm s^{-1}.

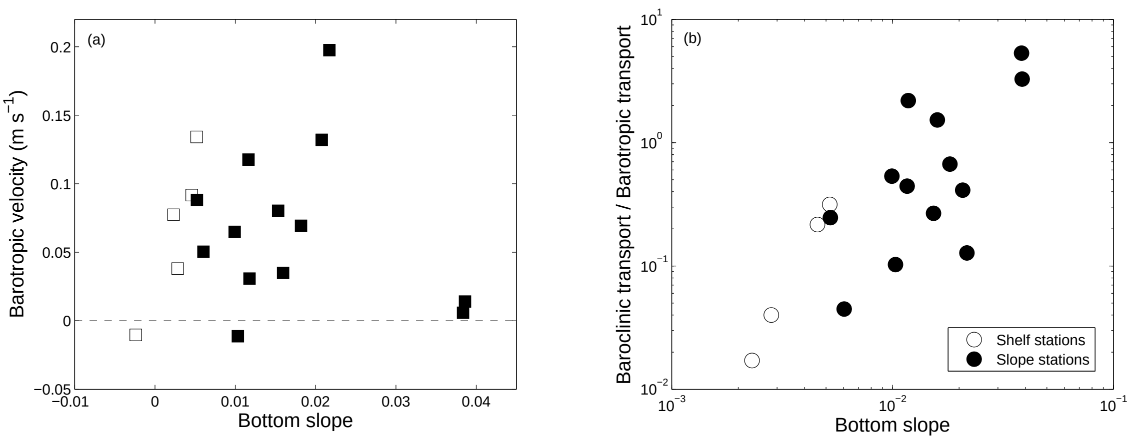

Figure 11: (*a*) Depth-averaged total geostrophic velocity plotted against steepness of the bottom topography. Open symbols indicate station pairs over the continental shelf, while solid symbols indicate stations pairs over the shelf break and continental slope. Positive slope indicates increasing depth with distance from shore. (*b*) Absolute value of the ratio of the depth-averaged geostrophic velocity, referenced to zero velocity at the deepest common level of each station pair, to the depth-averaged total geostrophic velocity, referenced to the LADCP data, plotted against steepness of the bottom topography.

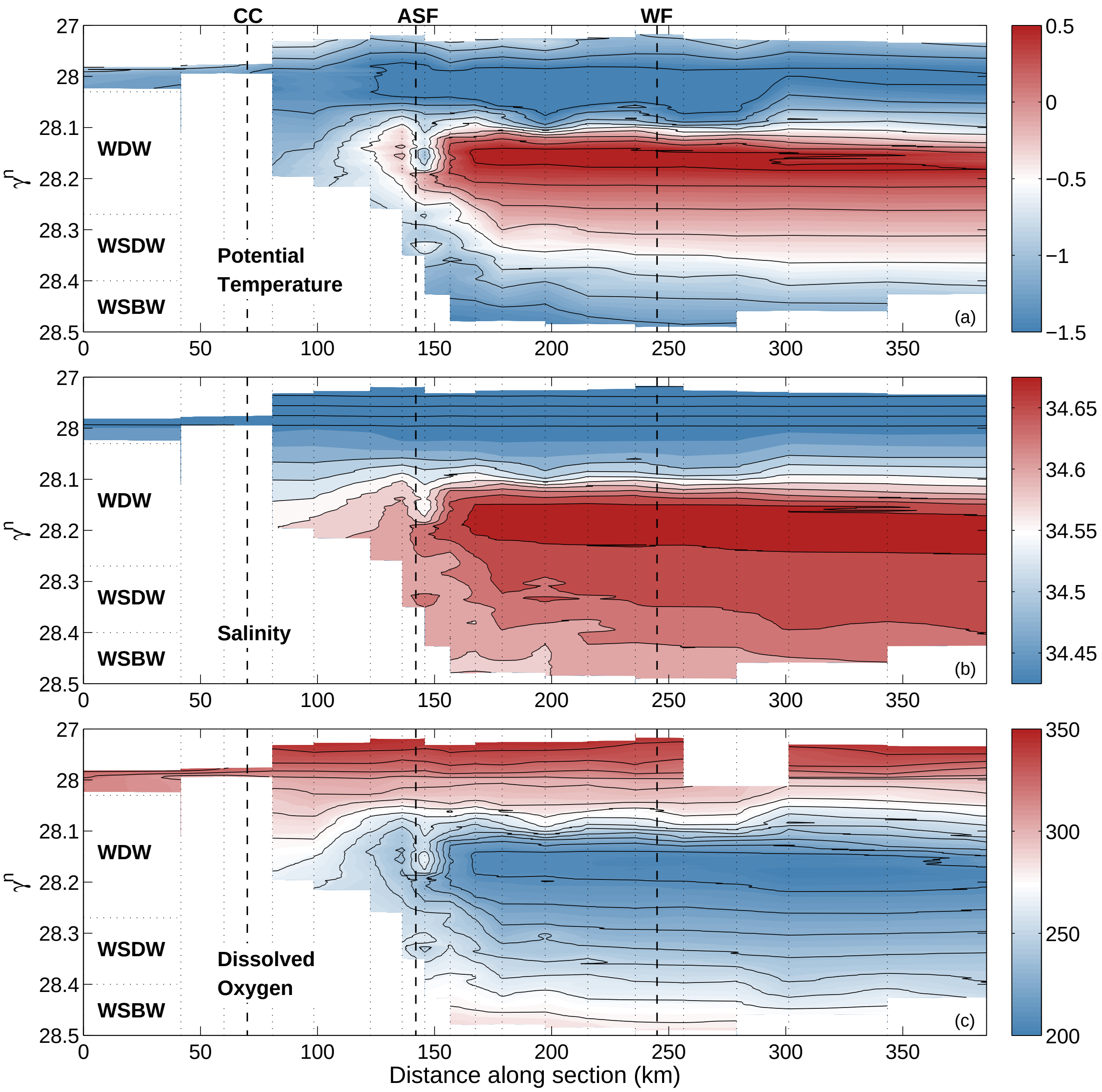

Figure 12: (a) Potential temperature (°C), (b) salinity and (c) dissolved oxygen (μmol kg^{-1}) along the ADELIE section contoured against neutral density γ^n as the ordinate. The contour intervals are 0.25°C and 10 μmol kg^{-1} in panels (a) and (c) respectively; in panel (b) contour intervals are 0.2 between 33.4 and 34.4 and 0.025 between 34.5 and 34.7. The dotted lines indicate the locations of the CTD profiles, and the dashed lines indicate the cores of the Antarctic Coastal Current (CC), the Antarctic Slope Front (ASF) and the Weddell Front (WF) as discussed in section **4.1**. Note the change in scale along the ordinate for $27 < \gamma^n < 28$.

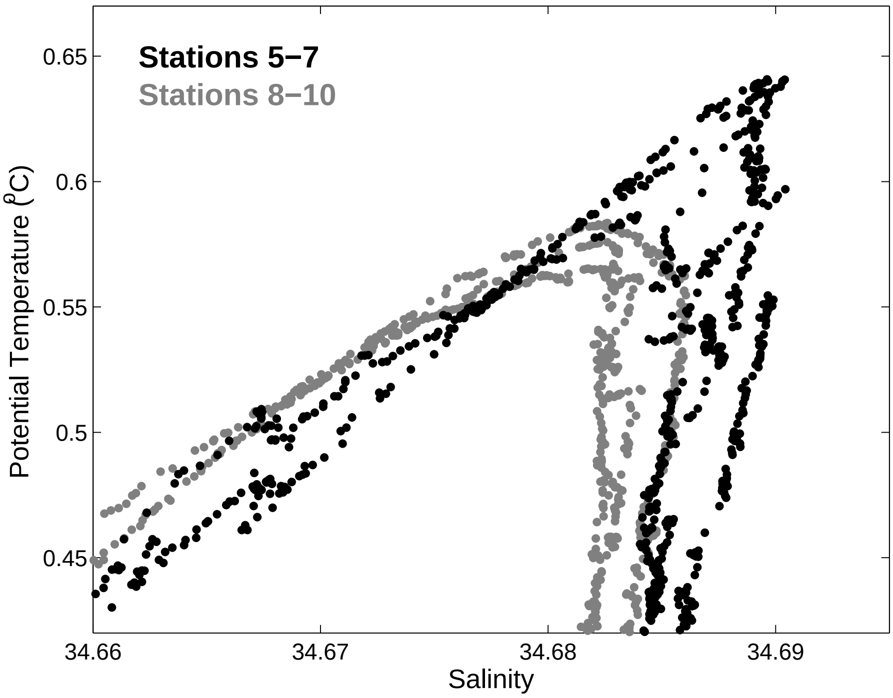

Figure 13: Potential temperature-salinity diagram near the WDW maxima. Properties in gray (black) are found shoreward (seaward) of the Weddell Front.

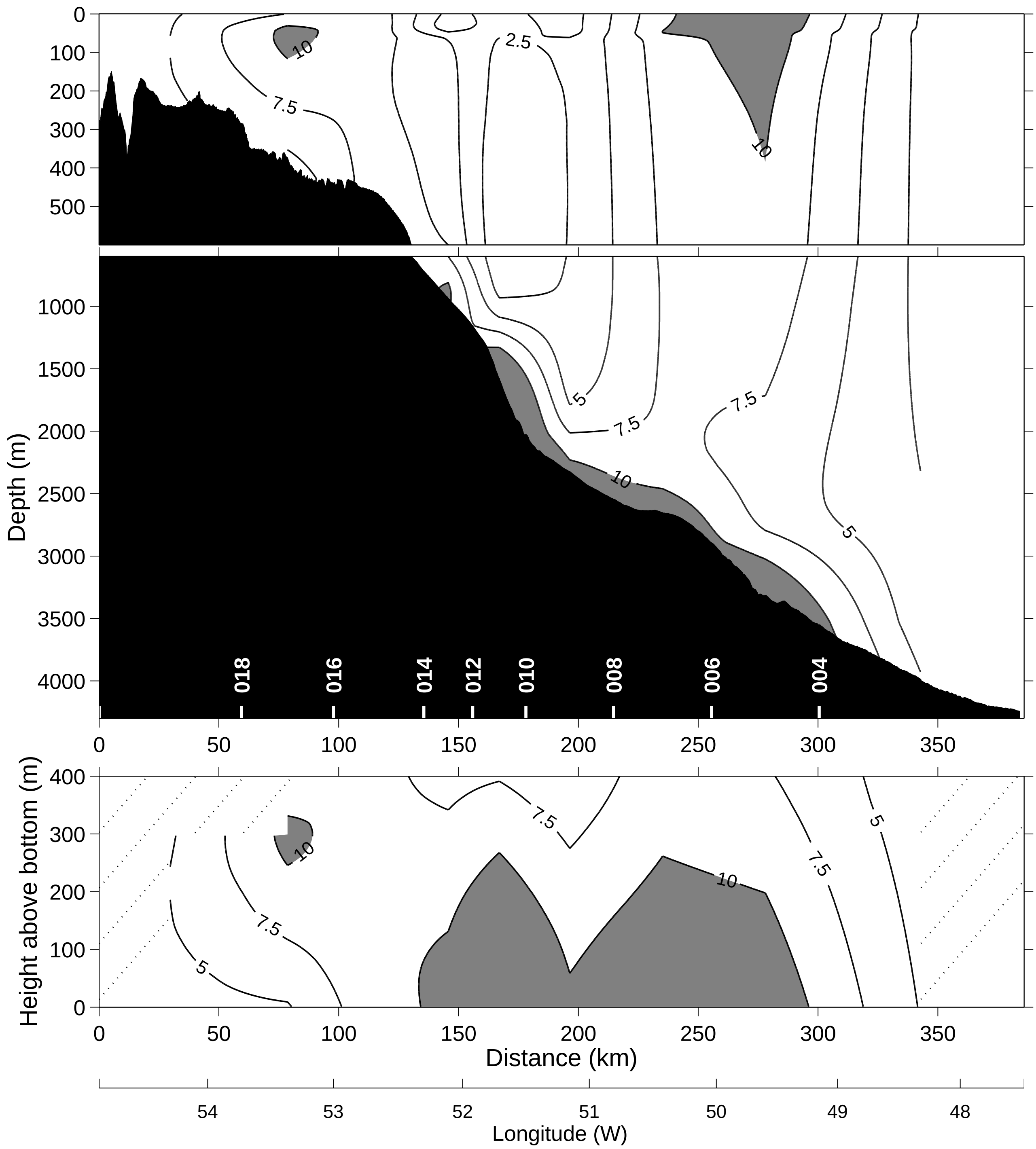

Figure 14: Sub-sampled total geostrophic velocities (cm s^{-1}) across the ADELIE section using only data from even-numbered stations. The geostrophic shear is referenced to the absolute velocity as determined from the LADCP measurements. The contours are every 2.5 cm s^{-1} between 2.5 and 10 cm s^{-1}. Otherwise as Figure 8.

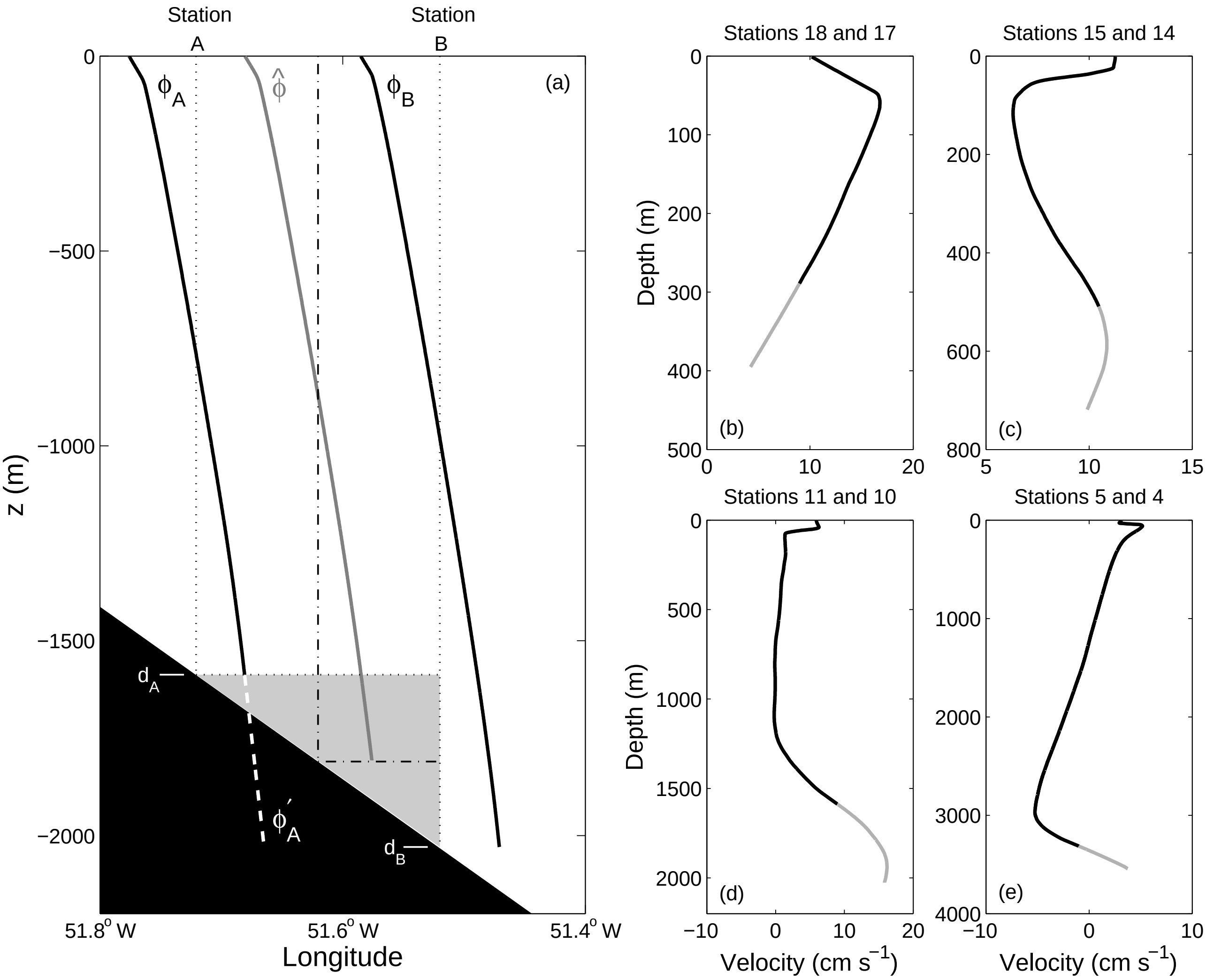

Figure 15: (a) Diagram depicting the method of bottom triangles as described in Appendix **A**. The sea bed is shaded black and the bottom triangle region is shaded light gray. The dotted lines indicate the positions of adjacent hydrographic stations A and B. The curves show profiles of geopotential anomaly ϕ (centered on their longitude position). The white dashed line ϕ'_A is a linear extrapolation of the ϕ_A curve to the depth of station B. The velocity across the horizontal level marked by the dashed-dotted line is calculated from the geopotential anomalies $\hat{\phi}$ and ϕ_B (see Appendix **A**). Panels (b) through (e) show examples from four station pairs of total geostrophic velocities above the deepest common level (black curves) along with the velocity estimates through the bottom triangles (gray curves).